REVISITING GENERATIVE POLICIES: A SIMPLER REINFORCEMENT LEARNING ALGORITHMIC PERSPECTIVE

Anonymous authors
Paper under double-blind review

ABSTRACT

Generative models, particularly diffusion models, have achieved remarkable success in density estimation for multimodal data, drawing significant interest from the reinforcement learning (RL) community, especially in policy modeling in continuous action spaces. However, existing works exhibit significant variations in training schemes and RL optimization objectives, and some methods are only applicable to diffusion models. In this study, we compare and analyze various generative policy training and deployment techniques, identifying and validating effective designs for generative policy algorithms. Specifically, we revisit existing training objectives and classify them into two categories, each linked to a simpler approach. The first approach, Generative Model Policy Optimization (GMPO), employs a native advantage-weighted regression formulation as the training objective, which is significantly simpler than previous methods. The second approach, Generative Model Policy Gradient (GMPG), offers a numerically stable implementation of the native policy gradient method. We introduce a standardized experimental framework named *GenerativeRL*. Our experiments demonstrate that the proposed methods achieve state-of-the-art performance on various offline-RL datasets, offering a unified and practical guideline for training and deploying generative policies.

1 INTRODUCTION

Generative models, such as flow models and diffusion models, have demonstrated remarkable capabilities in modeling multi-modal data across diverse applications, including image, video, and audio generation (Rombach et al., 2022; Ho et al., 2022; Mittal et al., 2021), and protein structure prediction (Abramson et al., 2024). Their expressive power stems from constructing continuous and invertible mappings between probability distributions, enabling the transformation of simple distributions like standard Gaussians into complex target distributions. Generative policies, which are RL policy models based on generative models, have become a focus of study within the RL community (Janner et al., 2022; Chi et al., 2023; Ren et al., 2024). They offer a principled approach to modeling expressive and nuanced action distributions, particularly important in robotics tasks with continuous and high-dimensional action spaces.

Despite the success of recent studies in offline-RL (Chen et al., 2023; Wang et al., 2023; Lu et al., 2023; Hansen-Estruch et al., 2023), these studies often employ complex training schemes and lack systematic investigation. This hinders understanding of key factors in training generative models for policy modeling, leading to unnecessary dependencies, training inefficiencies, and higher inference costs. Some work focuses primarily on diffusion models (Sohl-Dickstein et al., 2015; Ho et al., 2020), which has limited applicability to other generative models, such as flow models (Lipman et al., 2023; Liu et al., 2023; Pooladian et al., 2023; Albergo & Vanden-Eijnden, 2023; Tong et al., 2024).

This motivates us to develop simple yet effective training schemes for both diffusion and other emerging generative models, leveraging their advancements for the RL community's benefit. We revisit previous works on generative policy optimization in Table 1, and then categorize these works, and propose two training schemes: Generative Model Policy Optimization (GMPO) and Generative Model Policy Gradient (GMPG). GMPO is an advantage-weighted regression method with a stable training process that does not require pretraining the generative model before optimal policy extraction. This makes it more efficient and easier to train, featuring a shorter training schedule and a wider range of model applications while maintaining comparable performance to previous works. GMPG

is a policy gradient-based method in an RL-native formulation. We provide a numerically stable implementation for continuous-time generative models as an RL policy. It has proven effective in optimal policy extraction, especially for suboptimal policies. We evaluate the performance of diffusion and flow models using these two training schemes in an offline reinforcement learning setting with the D4RL dataset (Fu et al., 2021) and RL Unplugged (Gulcehre et al., 2020). Our results demonstrate that the proposed schemes offer comparable or better performance than previous works in most cases. We provide multiple ablations, covering model types, temperature settings, solver schemes, and sampling time steps for training, to validate the effectiveness of our proposed methods.

To facilitate consistent comparisons and analyses, we introduce a standardized experimental framework designed to combine the strengths of generative models and reinforcement learning by decoupling the generative model from the RL components. This decoupling enables consistent comparisons and analyses of different generative models within the same RL context, a capability lacking in previous works. Four key properties distinguish our framework from existing ones: unified API, flexible data formats and shapes, auto-grad support, and diverse generative model integration.

In conclusion, the main contributions of our work include:

- Proposing two simple yet effective RL-native training approaches for generative policies, GMPO and GMPG, which are compatible for both diffusion and flow models.
- Evaluating the performance of different generative models with the two training schemes on offline-RL dataset, achieving state-of-the-art performance in most cases. Our work elucidates the key factors in training generative policies and corrects several biases described in previous research.
- Providing a unified framework for combining the power of generative models and RL seamlessly, easy for conducting a fair and RL-native evaluations, named *GenerativeRL*.

2 Related Works

Generative Policy Algorithms. Haarnoja et al. (2017) introduces Soft Q-Learning and uses an energy-based generative policy for learning continuous actions from continuous states. Haarnoja et al. (2018a) integrates hierarchical policies with discrete layers into the Soft Actor-Critic (Haarnoja et al., 2018b) framework, which is called SACLSP and utilizes normalizing flows. Janner et al. (2022) first incorporate diffusion models into RL named as diffuser, acting as optimal trajectory planners by linking generative models with value function guidance being applied rudimentary. Chi et al. (2023) explores diffusion models for policy modeling in robotics, which is the concept of diffusion policy is first introduced. Chen et al. (2023) demonstrates effective policy learning in offline Q-learning using a diffusion model as support called SfBC. Wang et al. (2023) introduces Diffusion-QL and achieves policy regularization by alternating training between a Q-function-guided diffusion model and a diffusion-supported Q-function. Lu et al. (2023) introduces Q-guided Policy Optimization (QGPO) and derives the exact formulation of energy guidance for energy-conditioned diffusion models, enabling precise Q-guidance for optimal policy. Hansen-Estruch et al. (2023) introduces Implicit Diffusion Q-learning (IDQL) which uncovers the implicit policy form after Implicit Q-learning, emphasizing the importance of sampling from both the behavior policy and the diffusion model. Chen et al. (2024) uses the score function of a pre-trained diffusion model as a regularizer, optimizing a Gaussian policy to maximize the Q-function by combining the multimodal properties of diffusion models with the fast inference of Gaussian policies, which is called Score Regularized Policy Optimization (SRPO). Similar methods can also be applied to models trained using the flow matching (Zheng et al., 2023b; Kim et al., 2024). More details about the generative policy analyzed in this paper are provided in Appendix C.

Reinforcement Learning Frameworks. Several open-source RL frameworks provide unified interfaces for solving RL problems, although some are no longer maintained, such as OpenAI Baselines (Dhariwal et al., 2017), Facebook/ELF (Tian et al., 2017), TFAgents (Guadarrama et al., 2018), and JaxRL (Kostrikov, 2021). Active and widely-used frameworks include RLlib (Liang et al., 2018), which focuses on distributed RL for training large-scale models; Dopamine (Castro et al., 2018), a research framework for rapid RL algorithm prototyping; and Acme (Hoffman et al., 2020), designed for flexibility and scalability in RL research. Stable Baselines3 (Raffin et al., 2021), Tianshou (Weng et al., 2022), DI-engine (Niu et al., 2021), ElegantRL (Liu et al., 2021), and

CleanRL (Huang et al., 2022) offer a wide range of algorithms, environments, and user-friendly interfaces. TorchRL (Bou et al., 2023), a modular RL framework, supports PyTorch's native API and excels in handling dictionary-type tensors common in RL. The framework most related to ours is CleanDiffuser (Dong et al., 2024), which was recently proposed to integrate different types of diffusion algorithmic branches into a single framework.

3 BACKGROUND

This section provides a brief introduction to reinforcement learning and generative models. For more fundamentals of diffusion and flow models, please refer to Appendix B.

3.1 REINFORCEMENT LEARNING

Reinforcement learning (RL) addresses sequential decision-making tasks typically modeled as a Markov decision process (MDP), defined by the tuple $(\mathcal{S}, \mathcal{A}, p, r, \gamma)$. Here, $\mathcal{S}$ is the state space, $\mathcal{A}$ is the action space, $p(s_{t+1}|s_t, a_t)$ represents the transition dynamics, $r(s_t, a_t)$ is the reward function, and γ is the discount factor. At each time step t, the agent, in state s_t, takes an action $a_t \in \mathcal{A}$ according to the policy $\pi(a_t|s_t)$. The agent then receives a reward r_t and transitions to a new state s_{t+1} based on the transition dynamics $p(s_{t+1}|s_t, a_t)$. The goal of the agent is to learn a policy $\pi : \mathcal{S} \to \mathcal{A}$ that maximizes the expected cumulative reward over time, using only previously collected data. This objective can be expressed as: $\mathcal{R}_{s_0,a_0} = \mathbb{E}_{s_0,a_0,s_1,a_1,\dots}\left[\sum_{t=0}^{\infty} \gamma^t r_t\right]$.

In offline reinforcement learning (offline-RL), the agent has access to a fixed dataset $\mathcal{D}_\mu$ of historical interaction trajectories $\{s_t, a_t, r_t, s_{t+1}\}$, collected by a behavior policy $\mu(a_t|s_t)$, which is often suboptimal. Offline-RL is challenging because the agent cannot collect new data to correct its mistakes, unlike in online-RL, where exploration is possible.

Suppose the value of action a at state s is modeled by a Q-function $Q(s, a) \approx \mathcal{R}_{s,a}$, which estimates the expected return of taking action a at state s and following policy π thereafter. The value of state s is modeled by a V-function $V(s) = \mathbb{E}_{a\sim\pi(\cdot|s)}[Q(s, a)]$.

3.2 GENERATIVE MODELS

Diffusion Models. Given a fixed data or target distribution, a diffusion model is determined by the diffusion process path as an stochastic differential equation (SDE): $\mathrm{d}x = f(t)x_t\mathrm{d}t + g(t)\mathrm{d}w_t$. The transition distribution of a point $x \in \mathbb{R}^d$ from time 0 to t is: $p(x_t|x_0) \sim \mathcal{N}(x_t|\alpha_t x_0, \sigma_t^2 I)$. The reverse process path can be described by an ordinary differential equation (ODE):

$$\frac{\mathrm{d}x_t}{\mathrm{d}t} = v(x_t) = f(t)x_t - \frac{1}{2}g^2(t)\nabla_{x_t}\log p(x_t), \tag{1}$$

where $v(x_t)$ is the velocity function and $\nabla_{x_t}\log p(x_t)$ is the score function, typically modeled by a neural network with parameters θ, denoted as $v_\theta(x_t)$ and $s_\theta(x_t)$, respectively.

Flow Models. Consider a flow model with time-varying velocity $v(x_t)$, whose flow path can be described by an ODE: $\frac{\mathrm{d}x_t}{\mathrm{d}t} = v(x_t)$. The velocity field transforms the source distribution $p(x_0)$ at time $t = 0$ into the target distribution $p(x_1)$ at time $t = 1$ along the flow path and conforms to the continuity equation: $\frac{\partial p}{\partial t} + \nabla_x \cdot (pv) = 0$.

Model Training. Training continuous-time generative model involves a matching objective $\mathcal{L}_{\text{Matching}}(\theta)$, including the Score Matching method (Hyvärinen, 2005; Vincent, 2011):

$$\mathcal{L}_{\text{DSM}} = \frac{1}{2}\int_0^1 \mathbb{E}_{p(x_t,x_0)}\left[\lambda(t)\|s_\theta(x_t) - \nabla_{x_t}\log p(x_t|x_0)\|^2\right]\mathrm{d}t, \tag{2}$$

and the Flow Matching method (Lipman et al., 2023; Tong et al., 2024):

$$\mathcal{L}_{\text{CFM}} = \frac{1}{2}\int_0^1 \mathbb{E}_{p(x_t,x_0,x_1)}\left[\|v_\theta(x_t) - v(x_t|x_0, x_1)\|^2\right]\mathrm{d}t. \tag{3}$$

Table 1: Training schemes of different generative policy RL algorithms. The "Suitable Generative Model" column indicates the model types to which the algorithm can be applied, with parentheses showing the models actually used in previous work. If the model type is "Any," this method is applicable to all generative models, including diffusion and flow models discussed in this paper. The "Behavior Policy" column indicates whether the algorithm requires a pre-trained policy model for subsequent training. The "Critic Training" column describes the scheme used to learn the Q-function. The "Optimal Policy Extraction" column indicates whether the method trains and extracts the optimal policy.

Algorithm	Suitable Generative Model	Behavior Policy	Critic Training	Optimal Policy Extraction
SfBC	Any (VPSDE)	Needed	In-support Q-Learning	✗
QGPO	Diffusion (VPSDE)	Needed	In-support Q-Learning	✓
Diffusion-QL	Any (DDPM)	Needed	Conventional Q-Learning	✓
IDQL	Any (DDPM)	Needed	IQL	✗
SRPO	Diffusion (VPSDE)	Needed	IQL	✓
GMPO	Any	Not needed	IQL	✓
GMPG	Any	Needed	IQL	✓

For diffusion models, we investigate the Linear Variance-Preserving SDE (VP-SDE) model proposed by Song et al. (2021b), a continuous-time variant of Denoising Diffusion Probabilistic Models (DDPM) by Ho et al. (2020), and the Generalized VP-SDE (GVP) model introduced by Albergo & Vanden-Eijnden (2023), which extends the Improved DDPM by Nichol & Dhariwal (2021) with triangular scale and noise levels. For flow models, we investigate a simple flow model named I-CFM by Tong et al. (2024).

4 Revisiting Generative Policies

We establish the formulation of the optimal policy in offline-RL in Section 4.1. Next, we review prior work on generative policies in Section 4.2, with additional details in Appendix C. Subsequently, Section 4.3 introduces two straightforward and effective training schemes.

4.1 Optimal Policy in Offline-RL

Previous works in offline-RL (Peters & Schaal, 2007; Peters et al., 2010; Abdolmaleki et al., 2018; Wu et al., 2020) formulate policy optimization as a constrained optimization problem. The policy is learned by maximizing the expected return, subject to the KL divergence constraint to the behavior policy: $\pi^* = \arg\max_\pi \mathbb{E}_{s\sim\mathcal{D},a\sim\pi(\cdot|s)}\left[Q(s,a) - \frac{1}{\beta} D_{\mathrm{KL}}(\pi(\cdot|s)\|\mu(\cdot|s))\right]$. This approach ensures the learned policy rarely acts outside the support of the behavior policy, thus avoiding extrapolation errors that could degrade performance, as emphasized by Kumar et al. (2019) and Fujimoto et al. (2019). The optimal policy has an analytical form, as shown by Peng et al. (2021): $\pi^*(a|s) = \frac{e^{\beta(Q(s,a)-V(s))}}{Z(s)}\mu(a|s)$, where $Z(s)$ is a normalizing factor, and β is a temperature parameter. In practice, we can build a parameterized neural-net policy π_θ to approximate the optimal policy π^*. The policy model can be trained by minimizing the KL divergence:

$$\mathcal{L}(\theta) = \mathbb{E}_{s\sim\mathcal{D}}\left[D_{\mathrm{KL}}(\pi^*(\cdot|s)\|\pi_\theta(\cdot|s))\right] = \mathbb{E}_{s\sim\mathcal{D},a\sim\mu(\cdot|s)}\left[-\frac{e^{\beta(Q(s,a)-V(s))}}{Z(s)}\log\pi_\theta(a|s)\right] + C, \quad (4)$$

where C is a constant that does not depend on θ, or by using reverse KL divergence:

$$\mathcal{L}(\theta) = \mathbb{E}_{s\sim\mathcal{D}}\left[D_{\mathrm{KL}}(\pi_\theta(\cdot|s)\|\pi^*(\cdot|s))\right] = \mathbb{E}_{s\sim\mathcal{D},a\sim\pi_\theta(\cdot|s)}\left[-\beta Q(s,a) + D_{\mathrm{KL}}(\pi_\theta(\cdot|s)\|\mu(\cdot|s))\right] + C. \quad (5)$$

Comparison and derivation details of Eq. 4 and Eq. 5 are provided in Appendix A.

4.2 Previous Works on Generative Policy

Table 1 summarizes existing approaches for obtaining optimal generative policies. Table 2 provides an overview of the training and inference schemes of these algorithms.

Table 2: Generative model training and inference schemes of different generative RL algorithms. The forward KL method, which includes SfBC, QGPO, IDQL, and GMPO, incorporates an advantage-weighted regression term in its training or inference schemes. In contrast, the reverse KL method, including Diffusion-QL, SRPO, and GMPG, utilizes the Q-function for policy gradients with KL constraints. More comparisons are provided in Appendix A.2 and Appendix C.

Algorithm	Training Schemes	Inference Schemes
Forward KL	$\nabla_\theta \mathbb{E}_{s,a\sim\mu}\left[-\frac{e^{\beta(Q(s,a)-V(s))}}{Z(s)}\log \pi_\theta(a\|s)\right]$	
Reverse KL	$\nabla_\theta \mathbb{E}_{s,a\sim\pi_\theta}\left[-\beta Q(s,a) + D_{\mathrm{KL}}(\pi_\theta(\cdot\|s)\|\|\mu(\cdot\|s))\right]$	
Public Works		
SfBC	$\nabla_\theta \mathcal{L}_{\text{Matching}}(\theta)$ (Eq. 2)	$a \sim \text{softmax}_{a_i\sim\mu_\theta} Q(a_i, s)$
QGPO	$\nabla_\phi \mathbb{E}_{t,s,a_i\sim\mu}\left[-\frac{e^{\beta Q(s,a_i)}}{\sum_{i=1}^N e^{\beta Q(s,a_i)}}\log\frac{e^{\mathcal{E}_\phi(s,a_i,t)}}{\sum_{i=1}^N e^{\mathcal{E}_\phi(s,a_i,t)}}\right]$	$a \sim \pi, \nabla \log \pi = \nabla \log \mu + \nabla \log \mathcal{E}_\phi$
Diffusion-QL	$\nabla_\theta \mathbb{E}_{s,a\sim\pi_\theta}\left[-\beta Q(s,a) + \mathcal{L}_{\text{Matching}}(\theta)\right]$	$a \sim \text{softmax}_{a_i\sim\pi_\theta} Q(a_i, s)$
IDQL	$\nabla_\theta \mathcal{L}_{\text{Matching}}(\theta)$ (Eq. 2)	$a \sim \frac{\left\|\frac{\partial}{\partial V}(Q(s,a_i)-V(s))\right\|}{\|Q(s,a_i)-V(s)\|}\mu_\theta(a_i\|s)$
SRPO	$\nabla_\theta \mathbb{E}_{t,s,a\sim\pi_\theta}\left[-\beta Q(s,a) + w(t)(\epsilon_\psi(a_t\|s) - \epsilon)\right]$	$a \sim \pi_\theta$
This work		
GMPO	$\nabla_\theta \mathbb{E}_{s,a\sim\mu}\left[\frac{e^{\beta(Q(s,a)-V(s))}}{Z(s)}\mathcal{L}_{\text{Matching}}(\theta)\right]$	$a \sim \pi_\theta$
GMPG	$\nabla_\theta \mathbb{E}_{s,a\sim\pi_\theta}\left[-\beta Q(s,a) + \log\frac{\pi_\theta(a\|s)}{\mu(a\|s)}\right]$	$a \sim \pi_\theta$

- KL divergence or its variant for behavior policy constraint.
- Q function for policy gradient method.
- Importance weight for advantage-weighted regression.

Generative Model Type Table 1 highlights that QGPO and SRPO are limited to diffusion models, while other algorithms accommodate various generative models. QGPO's restriction arises from its reliance on the Contrastive Energy Prediction method (Eq. 30), which distills the Q function into an energy guidance model specifically designed for diffusion models (Appendix C.2). Similarly, SRPO's constraint stems from its score-regularized loss, which naturally aligns with diffusion models due to their inherent modeling of the score function. This compatibility, however, does not extend to non-diffusion models, such as flow models (see Appendix C.4 for further explanation).

Given the rapid advancements in generative modeling, we strive to establish a unified training scheme applicable to any generative model. By extracting effective designs from QGPO and SRPO algorithms, we can eliminate components that hinder generalization, training efficiency, and complexity without affecting performance

Behavior Policy Pretraining and Critic Training. As shown in Table 1, all methods require pretraining a behavior policy. SfBC and IDQL rely on it for importance sampling during inference. QGPO leverages the behavior policy for sampling in conjunction with energy guidance (Eq. 31). SRPO utilizes a well-trained behavior policy to regularize the Gaussian model policy (Eq35). Furthermore, while QGPO and SfBC employ in-support Q-learning with data augmentation from the behavior policy for Q function training (Eq. 29), Diffusion-QL utilizes traditional Q-learning with a similar dependence on the behavior policy (Eq. 36).

All three methods use the behavior policy for data augmentation during Q function training, making it essential. In contrast, SRPO and IDQL use Implicit Q-Learning to train the Q function directly (Eq. 32), without needing a behavior policy. This decouples the training of the behavior policy and the Q function, allowing simultaneous training.

The slower sampling rates of generative models raise questions about the necessity of data augmentation in training process of SfBC, QGPO, and Diffusion-QL. Simpler approaches, such as the Implicit Q-Learning employed by SRPO and IDQL, could offer greater efficiency for Q function training

in generative policy optimization. This observation motivates us to investigate whether comparable performance can be achieved by directly leveraging the Q function learned by IQL to guide generative policy optimization. Specifically, we are interested in exploring the potential of explicitly extracting a generative policy from the IQL-trained Q function, a direction not explored in previous works.

Optimal Policy Extraction. As shown in Table 1, SfBC and IDQL do not perform explicit policy extraction. Instead, they use importance sampling to derive the optimal policy from the behavior policy by evaluating the Q function. Although parallel computation can save inference time, the total computational budget during inference scales with the number of actions sampled from the behavior policy. SRPO uses a Gaussian model to explicitly output the optimal policy for guidance distillation, reducing computational costs and speeding up deployment. However, Gaussian models are generally less expressive than generative models, which can limit their effectiveness (Chi et al., 2023; Ren et al., 2024). Therefore, explicit policy extraction using generative models is preferred for balancing computational efficiency and expressiveness.

4.3 Generative Model Policy Training

To improve upon previous methods, we propose two straightforward yet effective training schemes for generative model policy optimization, derived from Eq. 4 and Eq. 5, as shown in Table 2. These schemes satisfy three key requirements: (1) Generality: Ensure compatibility with any generative model through a simple and effective training process. (2) Decoupled Training: Train the Q-function directly using Implicit Q-Learning (IQL), minimizing reliance on generative sampling. (3) Explicit Policy Extraction: Consistently infer only one action at a time for model inference.

Generative Model Policy Optimization. Inspired by Song et al. (2021a), who demonstrated that training with a maximum likelihood objective is equivalent to score matching, we replace the log-likelihood term with the matching loss (Eq. 2) of the generative model. By keeping the exponential form of the advantage function as the importance weight, as in Eq. 4, we derive the following advantage-weighted regression training objective suitable for both diffusion and flow models:

$$\begin{aligned}\mathcal{L}_{\text{GMPO}}(\theta) &= \mathbb{E}_{s\sim\mathcal{D},a\sim\pi^*(\cdot|s)}\left[\mathcal{L}_{\text{Matching}}(\theta)\right] \\ &= \mathbb{E}_{s\sim\mathcal{D},a\sim\mu(\cdot|s)}\left[\frac{e^{\beta(Q(s,a)-V(s))}}{Z(s)}\mathcal{L}_{\text{Matching}}(\theta)\right].\end{aligned} \tag{6}$$

Although Eq. 6 looks similar to Eq. 4, with the log-likelihood term replaced by the matching loss, it can be derived independently. See Appendix C.6 for more details.

Unlike previous works, our GMPO approach does not have to use data augmentation from the behavior policy. This removes the necessity of behavior policy and uses only data from the offline dataset:

$$\mathcal{L}_{\text{GMPO}}(\theta) = \mathbb{E}_{(s,a)\sim\mathcal{D}_\mu}\left[\frac{e^{\beta(Q(s,a)-V(s))}}{Z(s)}\mathcal{L}_{\text{Matching}}(\theta)\right]. \tag{7}$$

More details about GMPO are provided in Appendix C.6.

Generative Model Policy Gradient. This approach is directly derived from Eq. 5:

$$\begin{aligned}\mathcal{L}_{\text{GMPG}}(\theta) &= \mathbb{E}_{s\sim\mathcal{D}}\left[D_{\text{KL}}(\pi_\theta(\cdot|s)||\pi^*(\cdot|s))\right] \\ &= \mathbb{E}_{s\sim\mathcal{D},a\sim\pi_\theta(\cdot|s)}\left[-\beta Q(s,a) + D_{\text{KL}}(\pi_\theta(\cdot|s)||\mu(\cdot|s))\right] \\ &= \mathbb{E}_{s\sim\mathcal{D},a\sim\pi_\theta(\cdot|s)}\left[-\beta Q(s,a) + \log\pi_\theta(a|s) - \log\mu(a|s)\right].\end{aligned} \tag{8}$$

As an RL-native policy gradient method, GMPG directly calculates the log-likelihood term. However, efficiently computing gradients for diffusion and flow models is challenging due to their forward sampling process, which involves solving an initial value problem within an ODE solver. To address this, we employ advanced techniques such as the adjoint method or Neural ODEs (as proposed by Chen et al. (2018)), ensuring computational feasibility. Additionally, we utilize the Hutchinson trace estimator (Hutchinson, 1990; Grathwohl et al., 2019) to compute the log-likelihood of the policy for continuous-time generative models. See Appendix C.7.1 for more details.

In contrast to GMPG's direct log-likelihood calculation, Wang et al. (2023) propose an alternative approach that replaces the log-likelihood term with a score matching loss (Eq. 37), and further mitigates computational costs by employing a low time step ($T = 5$). However, this method has limitations, as it may not scale effectively to high-dimensional spaces and could potentially compromise generation quality with such a low time step. More details about GMPG are provided in Appendix C.7.

We illustrate the intuitive sampling trajectories of GMPO and GMPG with a 2D toy example in Appendix C.8 to clarify how it works.

5 FRAMEWORK

Based on the research needs analyzed in previous sections, we create *GenerativeRL* for verifying and comparing various generative models and reinforcement learning algorithms. The key distinction of GenerativeRL is its standardized implementation and unified API for generative models, allowing researchers to access these models at the configuration level without dealing with complex details. When compared to existing frameworks like CleanDiffuser (Dong et al., 2024), *GenerativeRL* differs in its design principles:

- Unified API: It offers a simple API that maximizes compatibility with different kinds of generative models, avoiding immature algorithms.
- Flexible Data Formats: It ensures consistent data formats for long-term use, supporting inputs and outputs as PyTorch tensors, tensordicts (Bou et al., 2023), and treetensors (Contributors, 2021), given the prevalence of dict-type data in RL.
- Auto-Grad Support: Designed to support Neural ODEs, it facilitates gradient-based inference via ODE or SDE, which is useful for many RL policies.
- Diverse Model Integration: It integrates various generative models, including flow and bridge models, treating diffusion models as a special case.

Thus, *GenerativeRL* seamlessly incorporates both diffusion and flow models for various RL algorithms, while decoupling the generative model from RL components. This allows for consistent comparisons and analyses of different generative models within the same RL context. See usage examples in Appendix E.1 and framework structure in Appendix E.2.

6 EXPERIMENTS

6.1 EXPERIMENTAL SETUP

Experiments are conducted on the classical offline-RL environments, D4RL dataset (Fu et al., 2021) and RL Unplugged DeepMind Control Suite datasets (Gulcehre et al., 2020).

Following QGPO (Lu et al., 2023), we adopt the same U-Net architecture with three hidden layers for all generative policy algorithms. The sampling process is performed using the Euler-Maruyama method in an ODE solver with uniform time steps, $T = 1000$ in training for GMPG, and $T = 32$ in evaluation for both GMPO and GMPG. All evaluations are conducted and averaged over five random seeds. Performance scores on D4RL datasets are normalized as suggested by Fu et al. (2021). We re-implemented QGPO, IDQL and SRPO under the same experimental settings for fair comparisons, reporting both our implementation scores and the original scores from the respective papers.

More details about computation resources, hyperparameters, and training specifics can be found in Appendix D.1.

6.2 EXPERIMENTS AND ANALYSIS

We address two key questions: (1) Can simpler RL-native training schemes like GMPO and GMPG extract the optimal policy and achieve performance comparable to state-of-the-art algorithms on the classical offline-RL dataset? (2) What are the experimental differences between GMPO and GMPG, given that both forward KL and reverse KL theoretically point to the same optimal policy?

Table 3: Performance evaluation on D4RL datasets of different generative policies. We provide the original scores of SfBC, Diffusion-QL, QGPO, IDQL, and SRPO from their respective papers. SfBC and Diffusion-QL are not integrated into our framework due to the substantial modifications required. Other algorithms have been successfully implemented using our unified framework. A detailed comparison between the original scores and our implementation can be found in Appendix D, Table 9.

Environment	**SfBC**	**Diffusion-QL**	**QGPO**	**IDQL**	**SRPO**	**GMPO**	**GMPG**
Model type **Function type**	**VPSDE** $\epsilon(x_t, t)$	**DDPM** $\epsilon(x_t, t)$	**VPSDE** $\epsilon(x_t, t)$	**VPSDE** $\epsilon(x_t, t)$	**VPSDE** $\epsilon(x_t, t)$	**GVP** $v(x_t, t)$	**VPSDE** $v(x_t, t)$
Pretrain scheme **Fintune scheme**	Eq. 2 /	Eq. 2 Eq. 37	Eq. 2 Eq. 30	Eq. 2 /	Eq. 2 Eq. 35	/ Eq. 40	Eq. 3 Eq. 8
halfcheetah-medium-expert-v2	92.6	96.8	92.0 ± 1.5	91.7 ± 2.4	86.7 ± 3.7	91.9 ± 3.2	89.0 ± 6.4
hopper-medium-expert-v2	108.6	111.1	107.0 ± 0.9	96.8 ± 10.4	100.8 ± 9.3	112.0 ± 1.8	107.8 ± 1.9
walker2d-medium-expert-v2	109.8	110.1	107.3 ± 1.3	107.0 ± 0.5	118.7 ± 1.4	108.1 ± 0.7	112.8 ± 1.2
halfcheetah-medium-v2	45.9	51.1	44.0 ± 0.7	43.7 ± 2.8	51.4 ± 2.9	49.9 ± 2.7	57.0 ± 3.1
hopper-medium-v2	57.1	90.5	80.1 ± 7.0	72.1 ± 17.6	97.2 ± 3.3	74.6 ± 21.2	101.1 ± 2.6
walker2d-medium-v2	77.9	87.0	82.8 ± 2.7	82.0 ± 2.4	85.6 ± 2.1	81.1 ± 4.3	91.9 ± 0.9
halfcheetah-medium-replay-v2	37.1	47.8	42.5 ± 1.7	41.6 ± 8.4	47.2 ± 4.5	42.3 ± 3.6	50.5 ± 2.7
hopper-medium-replay-v2	86.2	100.7	99.3 ± 1.8	89.1 ± 3.1	78.2 ± 12.1	97.8 ± 3.8	86.3 ± 10.5
walker2d-medium-replay-v2	65.1	95.5	81.1 ± 4.2	80.4 ± 9.2	79.6 ± 7.6	86.4 ± 1.7	90.1 ± 2.2
Average (Locomotion)	75.6	88.0	81.8 ± 2.4	78.3 ± 6.3	82.8 ± 5.1	82.7 ± 4.8	87.3 ± 3.5

Table 3 shows the performance of various generative policy algorithms on D4RL environments, including SfBC (Chen et al., 2023), Diffusion-QL (Wang et al., 2023), QGPO (Lu et al., 2023), IDQL (Hansen-Estruch et al., 2023), and SRPO (Chen et al., 2024). Table 4 presents the performance of generative policies on the RL Unplugged DeepMind Control Suite datasets (Gulcehre et al., 2020). For reference, we include the performance of two classical offline RL algorithms: RABM (Siegel et al., 2020) and D4PG (Barth-Maron et al., 2018), the latter being the algorithm for which most of this dataset was collected. The average performance across these tasks demonstrates that GMPO and GMPG effectively solve challenging continuous control tasks, achieving competitive results compared with other state-of-the-art algorithms.

Hansen-Estruch et al. (2023) claims that using highly expressive models with importance weighted objectives can be problematic as such models can increase the likelihood of all training points regardless of their weight. And they find using advantage-weighted regression in the DDPM objective to not help performance, so they recommend sampling from behavior policy and filter out the high Q-value actions with the softmax importance sampling. However, our practice overturns the above claims and found that generative policy trained with advantage-weighted regression even from a scratch initialization can gain comparably equivalent performance to IDQL using resampling tricks, as shown in Table 3. Since utilizing the same Implicit Q-learning method, GMPO and GMPG both successfully extract optimal policies from the Q function. GMPO, a simpler variant of QGPO, achieves comparable performance on these datasets. This indicates that the advantage-weighted regression loss, a common component of both methods, is crucial for successful training.

Unlike Diffusion-QL, which separates the KL divergence into a simulation-free score matching loss but remains Q guidance through simulation, GMPG computes both Q guidance and the KL divergence directly through simulation, achieving similar performance. Despite using a significantly larger number of sampling steps ($T = 1000$) compared to Diffusion-QL ($T = 5$), GMPG does not exhibit computational difficulties in our implementation. This effectively addresses the limitations highlighted by Wang et al. (2023), where the maximum T they could afford was 20, and they opted for $T = 5$ to balance performance and computational cost.

In addition, our experiments challenged the intuition that a complete 1000-step inference inherently leads to high computational costs, even with Neural ODEs. Our results demonstrate that with direct gradient guidance, no extra computational cost is required for optimization. For example, in halfcheetah-medium-v2-GMPG-GVP, optimal performance is achieved in 50-100 steps, taking 5-10 hours on an A100 GPU. Similarly, for halfcheetah-medium-v2-GMPO-GVP, optimal performance occurs at 240K-480K steps, also requiring 5-10 hours. Despite slower calculations for a 1000-step inference for one gradient step, it uses fewer training batches, resulting in similar overall time costs, ensuring no computation is wasted during training.

Table 4: Performance evaluation on RL Unplugged DeepMind Control Suite dataset of different generative policies. We evaluate different generative policies using the RL Unplugged DeepMind Control Suite dataset. D4PG is the primary algorithm used for most of this dataset's collection, while RABM serves as a classical offline-RL algorithm for comparison. We present the original scores of D4PG and RABM from their respective papers. Since the original papers for QGPO, IDQL, and SRPO do not provide performance metrics on this dataset, we report the scores from our implementations.

Environment	**D4PG**	**RABM**	**QGPO**	**IDQL**	**SRPO**	**GMPO**	**GMPG**
Model type	/	/	**VPSDE**	**VPSDE**	**VPSDE**	**GVP**	**GVP**
Function type	/	/	$\epsilon(x_t, t)$	$\epsilon(x_t, t)$	$\epsilon(x_t, t)$	$v(x_t, t)$	$v(x_t, t)$
Pretrain scheme	/	/	Eq. 2	Eq. 2	Eq. 2	/	Eq. 3
Fintune scheme	/	/	Eq. 30	/	Eq. 35	Eq. 40	Eq. 8
Cartpole swingup	856 ± 13	798 ± 31	806 ± 54	851 ± 9	842 ± 13	830 ± 36	858 ± 51
Cheetah run	308 ± 122	304 ± 32	338 ± 135	451 ± 231	344 ± 127	359 ± 188	503 ± 212
Humanoid run	1.72 ± 1.66	303 ± 6	245 ± 45	179 ± 91	242 ± 22	226 ± 72	209 ± 61
Manipulator insert ball	154 ± 55	409 ± 5	340 ± 451	308 ± 433	352 ± 458	402 ± 489	686 ± 341
Walker stand	930 ± 46	689 ± 14	672 ± 266	850 ± 161	946 ± 23	593 ± 287	771 ± 292
Finger turn hard	714 ± 80	433 ± 3	698 ± 352	534 ± 417	328 ± 464	738 ± 204	657 ± 371
Fish swim	180 ± 55	504 ± 13	412 ± 297	474 ± 248	597 ± 356	634 ± 192	515 ± 168
Manipulator insert peg	50.4 ± 9.2	290 ± 15	279 ± 229	314 ± 376	327 ± 383	398 ± 481	540 ± 343
Walker walk	549 ± 366	651 ± 8	791 ± 150	887 ± 51	963 ± 15	869 ± 241	656 ± 233
Average	416 ± 83	487 ± 14	509 ± 220	538 ± 224	549 ± 207	561 ± 243	599 ± 230

Figure 1 illustrates the log-likelihood of D4RL datasets evaluated by GMPO/GMPG policies across different training iterations. A higher log-likelihood indicates that the generative model output is closer to the original data distribution. For hopper-medium-v2, the generative model trained with GMPO maintains a certain distance from the original data distribution throughout training. In contrast, the GMPG-trained model closely aligns with the original data distribution during pretraining but diverges more during finetuning compared to GMPO. This divergence allows GMPG to achieve better performance. In the case of halfcheetah-medium-expert-v2, both GMPO and GMPG benefit from high-quality data, as the optimal policy is already near the original distribution. Here, GMPO excels in filtering out high Q-value actions, resulting in a slightly better performance compared to GMPG.

More experiment details for GMPO and GMPG on D4RL AntMaze dataset can be found in Table 11 (Appendix D).

In general, GMPG with reverse KL loss outperforms GMPO and other generative policies with Forward KL loss in most medium and medium-replay locomotion tasks. This suggests that the policy gradient method more aggressively leverages Q guidance and is less constrained by the behavior policy, allowing optimization into regions with less data support — a beneficial exploration strategy in medium and medium-replay data, though it results in slightly poorer performance with expert data as shown in Table 3. Additionally, GMPO shows more stable training convergence with monotonic improvement, while GMPG exhibits fluctuating performance during training with small batch sizes, requiring larger batch sizes for stability.

6.3 Ablation Experiments

Generative Model Type. Table 5 presents a performance comparison of three generative models: GVP, VPSDE, and I-CFM (a more detailed comparison is available in Table 10). Overall, all three models demonstrate comparable performance. However, I-CFM exhibits slightly weaker performance in certain cases. This discrepancy may stem from its simpler flow path, as defined in Eq. 28, which could potentially limit its ability to capture the environment's complex dynamics effectively.

Sampling Scheme for GMPG. As shown in Table 6, our ablation study reveals that increasing the number of sampling time steps T within the GMPG algorithm can lead to improved performance.

Further ablation experiments about temperature coefficient β and solver schemes for sampling are detailed in Appendix D.3.

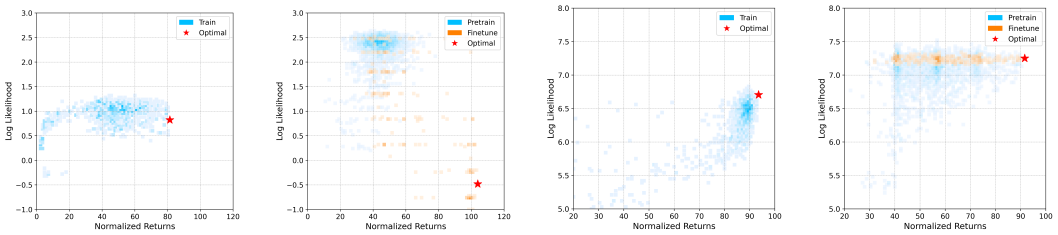

(a) HM/GMPO-GVP (b) HM/GMPG-GVP (c) HME/GMPO-GVP (d) HME/GMPG-GVP

Figure 1: Log-Likelihood of D4RL datasets evaluated by GMPO/GMPG-GVP policies during training. HM stands for hopper-medium-v2, HME stands for halfcheetah-medium-expert-v2. Each point represents a model during training, with colors indicating different stages. The returns of the model are evaluated and averaged over five random seeds. Blue points denote the pretraining stage for GMPG and the training stage for GMPO, as GMPO does not require pretraining. Orange points indicate the finetuning stage for GMPG. The star marker shows the optimal model obtained during training. The density of the points reflects the number of models in that area.

Table 5: Performance comparison of model types on D4RL datasets. The average performance is calculated over 9 locomotion tasks.

Algo. type	**GMPO**			**GMPG**		
Model type	**VPSDE**	**GVP**	**I-CFM**	**VPSDE**	**GVP**	**I-CFM**
Average (Locomotion)	80.2 ± 4.2	82.7 ± 4.8	76.2 ± 8.0	87.3 ± 3.5	84.2 ± 3.2	83.4 ± 4.2

Table 6: Performance comparison of different sampling time steps for GMPG. The time span of the ODE solver is $[0, 1]$, so a larger T means more sampling steps and a smaller step size.

Pretrain scheme / Finetune scheme	**GMPG / VPSDE /** $v(x_t, t)$ Eq. 3 / Eq. 8		
T **(Used for Training Only)**	32	100	1000
halfcheetah-medium-v2	53.9 ± 2.7	55.8 ± 2.8	57.0 ± 3.1
halfcheetah-medium-replay-v2	43.4 ± 3.5	49.1 ± 3.3	50.5 ± 2.7

7 Conclusion

In this paper, we provide a comprehensive study of generative policies and propose two unified and RL-native training schemes, GMPO and GMPG, that are effective and straightforward for both diffusion and flow models. GMPO benefits from a stable training process and does not require pretraining the generative model before optimal policy extraction, making it more efficient and easier to train. GMPG is a native policy gradient-based method for continuous-time generative models, and we provide a numerically stable implementation for the RL community. Our experiment results demonstrate that the proposed training schemes offer comparable or better performance than previous works in most cases.

To ensure consistent comparisons and analyses, we introduce a unified framework for reinforcement learning algorithms that leverages the expressive power of generative models. This standardized experimental framework decouples the generative model from the RL components, allowing for consistent evaluation of different generative models within the same RL context.

Overall, this work simplifies and unifies the training of generative models for policy modeling, providing practical guidelines for training and deploying generative policies in reinforcement learning. Additionally, we discuss existing limitations and valuable topics for future work in Appendix F.

REFERENCES

Abbas Abdolmaleki, Jost Tobias Springenberg, Yuval Tassa, Remi Munos, Nicolas Heess, and Martin Riedmiller. Maximum a posteriori policy optimisation. In *International Conference on Learning Representations*, 2018. URL https://openreview.net/forum?id=S1ANxQW0b.

Josh Abramson, Jonas Adler, Jack Dunger, Richard Evans, Tim Green, Alexander Pritzel, Olaf Ronneberger, Lindsay Willmore, Andrew J Ballard, Joshua Bambrick, et al. Accurate structure prediction of biomolecular interactions with alphafold 3. *Nature*, pp. 1–3, 2024.

Michael Samuel Albergo and Eric Vanden-Eijnden. Building normalizing flows with stochastic interpolants. In *The Eleventh International Conference on Learning Representations*, 2023. URL https://openreview.net/forum?id=li7qeBbCR1t.

Gabriel Barth-Maron, Matthew W Hoffman, David Budden, Will Dabney, Dan Horgan, Dhruva Tb, Alistair Muldal, Nicolas Heess, and Timothy Lillicrap. Distributed distributional deterministic policy gradients. *arXiv preprint arXiv:1804.08617*, 2018.

Jagdeep Bhatia, Holly Jackson, Yunsheng Tian, Jie Xu, and Wojciech Matusik. Evolution gym: A large-scale benchmark for evolving soft robots. *Advances in Neural Information Processing Systems*, 34, 2021.

Albert Bou, Matteo Bettini, Sebastian Dittert, Vikash Kumar, Shagun Sodhani, Xiaomeng Yang, Gianni De Fabritiis, and Vincent Moens. Torchrl: A data-driven decision-making library for pytorch, 2023.

Pablo Samuel Castro, Subhodeep Moitra, Carles Gelada, Saurabh Kumar, and Marc G. Bellemare. Dopamine: A Research Framework for Deep Reinforcement Learning. 2018. URL http://arxiv.org/abs/1812.06110.

Huayu Chen, Cheng Lu, Chengyang Ying, Hang Su, and Jun Zhu. Offline reinforcement learning via high-fidelity generative behavior modeling. In *The Eleventh International Conference on Learning Representations*, 2023. URL https://openreview.net/forum?id=42zs3qa2kpy.

Huayu Chen, Cheng Lu, Zhengyi Wang, Hang Su, and Jun Zhu. Score regularized policy optimization through diffusion behavior. In *The Twelfth International Conference on Learning Representations*, 2024. URL https://openreview.net/forum?id=xCRr9DrolJ.

Ricky T. Q. Chen, Yulia Rubanova, Jesse Bettencourt, and David K Duvenaud. Neural ordinary differential equations. In S. Bengio, H. Wallach, H. Larochelle, K. Grauman, N. Cesa-Bianchi, and R. Garnett (eds.), *Advances in Neural Information Processing Systems*, volume 31. Curran Associates, Inc., 2018. URL https://proceedings.neurips.cc/paper_files/paper/2018/file/69386f6bb1dfed68692a24c8686939b9-Paper.pdf.

Cheng Chi, Siyuan Feng, Yilun Du, Zhenjia Xu, Eric A. Cousineau, Benjamin Burchfiel, and Shuran Song. Diffusion policy: Visuomotor policy learning via action diffusion. *ArXiv*, abs/2303.04137, 2023. URL https://api.semanticscholar.org/CorpusID:257378658.

OpenDILab Contributors. Treetensor: a generalized tree-based tensor structure. https://github.com/opendilab/DI-treetensor, 2021.

Prafulla Dhariwal, Christopher Hesse, Oleg Klimov, Alex Nichol, Matthias Plappert, Alec Radford, John Schulman, Szymon Sidor, Yuhuai Wu, and Peter Zhokhov. Openai baselines. https://github.com/openai/baselines, 2017.

Zibin Dong, Yifu Yuan, Jianye Hao, Fei Ni, Yi Ma, Pengyi Li, and Yan Zheng. Cleandiffuser: An easy-to-use modularized library for diffusion models in decision making. *arXiv preprint arXiv:2406.09509*, 2024.

Chris Finlay, Joern-Henrik Jacobsen, Levon Nurbekyan, and Adam Oberman. How to train your neural ODE: the world of Jacobian and kinetic regularization. In Hal Daumé III and Aarti Singh (eds.), *Proceedings of the 37th International Conference on Machine Learning*, volume 119 of *Proceedings of Machine Learning Research*, pp. 3154–3164. PMLR, 13–18 Jul 2020. URL https://proceedings.mlr.press/v119/finlay20a.html.

Justin Fu, Aviral Kumar, Ofir Nachum, George Tucker, and Sergey Levine. D4{rl}: Datasets for deep data-driven reinforcement learning, 2021. URL https://openreview.net/forum?id=px0-N3_KjA.

Scott Fujimoto, David Meger, and Doina Precup. Off-policy deep reinforcement learning without exploration. In Kamalika Chaudhuri and Ruslan Salakhutdinov (eds.), *Proceedings of the 36th International Conference on Machine Learning*, volume 97 of *Proceedings of Machine Learning Research*, pp. 2052–2062. PMLR, 09–15 Jun 2019. URL https://proceedings.mlr.press/v97/fujimoto19a.html.

Will Grathwohl, Ricky T. Q. Chen, Jesse Bettencourt, and David Duvenaud. Scalable reversible generative models with free-form continuous dynamics. In *International Conference on Learning Representations*, 2019. URL https://openreview.net/forum?id=rJxgknCcK7.

Sergio Guadarrama, Anoop Korattikara, Oscar Ramirez, Pablo Castro, Ethan Holly, Sam Fishman, Ke Wang, Ekaterina Gonina, Neal Wu, Efi Kokiopoulou, Luciano Sbaiz, Jamie Smith, Gábor Bartók, Jesse Berent, Chris Harris, Vincent Vanhoucke, and Eugene Brevdo. TF-Agents: A library for reinforcement learning in tensorflow. https://github.com/tensorflow/agents, 2018. URL https://github.com/tensorflow/agents. [Online; accessed 25-June-2019].

Caglar Gulcehre, Ziyu Wang, Alexander Novikov, Thomas Paine, Sergio Gómez, Konrad Zolna, Rishabh Agarwal, Josh S Merel, Daniel J Mankowitz, Cosmin Paduraru, et al. Rl unplugged: A suite of benchmarks for offline reinforcement learning. *Advances in Neural Information Processing Systems*, 33:7248–7259, 2020.

Tuomas Haarnoja, Haoran Tang, Pieter Abbeel, and Sergey Levine. Reinforcement learning with deep energy-based policies. In *Proceedings of the 34th International Conference on Machine Learning - Volume 70*, ICML'17, pp. 1352–1361. JMLR.org, 2017.

Tuomas Haarnoja, Kristian Hartikainen, Pieter Abbeel, and Sergey Levine. Latent space policies for hierarchical reinforcement learning. In Jennifer Dy and Andreas Krause (eds.), *Proceedings of the 35th International Conference on Machine Learning*, volume 80 of *Proceedings of Machine Learning Research*, pp. 1851–1860. PMLR, 10–15 Jul 2018a. URL https://proceedings.mlr.press/v80/haarnoja18a.html.

Tuomas Haarnoja, Aurick Zhou, Pieter Abbeel, and Sergey Levine. Soft actor-critic: Off-policy maximum entropy deep reinforcement learning with a stochastic actor. In Jennifer Dy and Andreas Krause (eds.), *Proceedings of the 35th International Conference on Machine Learning*, volume 80 of *Proceedings of Machine Learning Research*, pp. 1861–1870. PMLR, 10–15 Jul 2018b. URL https://proceedings.mlr.press/v80/haarnoja18b.html.

Philippe Hansen-Estruch, Ilya Kostrikov, Michael Janner, Jakub Grudzien Kuba, and Sergey Levine. IDQL: implicit q-learning as an actor-critic method with diffusion policies. *CoRR*, abs/2304.10573, 2023. doi: 10.48550/ARXIV.2304.10573. URL https://doi.org/10.48550/arXiv.2304.10573.

Jonathan Ho, Ajay Jain, and Pieter Abbeel. Denoising diffusion probabilistic models. In H Larochelle, M Ranzato, R Hadsell, M F Balcan, and H Lin (eds.), *Advances in Neural Information Processing Systems*, volume 33, pp. 6840–6851. Curran Associates, Inc., 2020. URL https://proceedings.neurips.cc/paper_files/paper/2020/file/4c5bcfec8584af0d967f1ab10179ca4b-Paper.pdf.

Jonathan Ho, Tim Salimans, Alexey Gritsenko, William Chan, Mohammad Norouzi, and David J Fleet. Video diffusion models. In S. Koyejo, S. Mohamed, A. Agarwal, D. Belgrave, K. Cho, and A. Oh (eds.), *Advances in Neural Information Processing Systems*, volume 35, pp. 8633–8646. Curran Associates, Inc., 2022. URL https://proceedings.neurips.cc/paper_files/paper/2022/file/39235c56aef13fb05a6adc95eb9d8d66-Paper-Conference.pdf.

Matthew W. Hoffman, Bobak Shahriari, John Aslanides, Gabriel Barth-Maron, Nikola Momchev, Danila Sinopalnikov, Piotr Stańczyk, Sabela Ramos, Anton Raichuk, Damien Vincent, Léonard

Hussenot, Robert Dadashi, Gabriel Dulac-Arnold, Manu Orsini, Alexis Jacq, Johan Ferret, Nino Vieillard, Seyed Kamyar Seyed Ghasemipour, Sertan Girgin, Olivier Pietquin, Feryal Behbahani, Tamara Norman, Abbas Abdolmaleki, Albin Cassirer, Fan Yang, Kate Baumli, Sarah Henderson, Abe Friesen, Ruba Haroun, Alex Novikov, Sergio Gómez Colmenarejo, Serkan Cabi, Caglar Gulcehre, Tom Le Paine, Srivatsan Srinivasan, Andrew Cowie, Ziyu Wang, Bilal Piot, and Nando de Freitas. Acme: A research framework for distributed reinforcement learning. *arXiv preprint arXiv:2006.00979*, 2020. URL https://arxiv.org/abs/2006.00979.

Shengyi Huang, Rousslan Fernand Julien Dossa, Chang Ye, Jeff Braga, Dipam Chakraborty, Kinal Mehta, and João G.M. Araújo. Cleanrl: High-quality single-file implementations of deep reinforcement learning algorithms. *Journal of Machine Learning Research*, 23(274):1–18, 2022. URL http://jmlr.org/papers/v23/21-1342.html.

M.F. Hutchinson. A stochastic estimator of the trace of the influence matrix for laplacian smoothing splines. *Communications in Statistics - Simulation and Computation*, 19(2):433–450, 1990. doi: 10.1080/03610919008812866. URL https://doi.org/10.1080/03610919008812866.

Aapo Hyvärinen. Estimation of non-normalized statistical models by score matching. *Journal of Machine Learning Research*, 6(24):695–709, 2005. URL http://jmlr.org/papers/v6/hyvarinen05a.html.

Michael Janner, Yilun Du, Joshua Tenenbaum, and Sergey Levine. Planning with diffusion for flexible behavior synthesis. In Kamalika Chaudhuri, Stefanie Jegelka, Le Song, Csaba Szepesvari, Gang Niu, and Sivan Sabato (eds.), *Proceedings of the 39th International Conference on Machine Learning*, volume 162 of *Proceedings of Machine Learning Research*, pp. 9902–9915. PMLR, 17–23 Jul 2022. URL https://proceedings.mlr.press/v162/janner22a.html.

Tero Karras, Miika Aittala, Timo Aila, and Samuli Laine. Elucidating the design space of diffusion-based generative models. In Alice H. Oh, Alekh Agarwal, Danielle Belgrave, and Kyunghyun Cho (eds.), *Advances in Neural Information Processing Systems*, 2022. URL https://openreview.net/forum?id=k7FuTOWMOc7.

Minu Kim, Yongsik Lee, Sehyeok Kang, Jihwan Oh, Song Chong, and Se-Young Yun. Preference alignment with flow matching. *arXiv preprint arXiv:2405.19806*, 2024.

Ilya Kostrikov. JAXRL: Implementations of Reinforcement Learning algorithms in JAX, 10 2021. URL https://github.com/ikostrikov/jaxrl.

Aviral Kumar, Justin Fu, Matthew Soh, George Tucker, and Sergey Levine. Stabilizing off-policy q-learning via bootstrapping error reduction. In H. Wallach, H. Larochelle, A. Beygelzimer, F. d'Alché-Buc, E. Fox, and R. Garnett (eds.), *Advances in Neural Information Processing Systems*, volume 32. Curran Associates, Inc., 2019. URL https://proceedings.neurips.cc/paper_files/paper/2019/file/c2073ffa77b5357a498057413bb09d3a-Paper.pdf.

Eric Liang, Richard Liaw, Robert Nishihara, Philipp Moritz, Roy Fox, Ken Goldberg, Joseph E. Gonzalez, Michael I. Jordan, and Ion Stoica. RLlib: Abstractions for distributed reinforcement learning. In *International Conference on Machine Learning (ICML)*, 2018.

Yaron Lipman, Ricky T. Q. Chen, Heli Ben-Hamu, Maximilian Nickel, and Matthew Le. Flow matching for generative modeling. In *The Eleventh International Conference on Learning Representations*, 2023. URL https://openreview.net/forum?id=PqvMRDCJT9t.

Xiao-Yang Liu, Zechu Li, Ming Zhu, Zhaoran Wang, and Jiahao Zheng. ElegantRL: Massively parallel framework for cloud-native deep reinforcement learning. https://github.com/AI4Finance-Foundation/ElegantRL, 2021.

Xingchao Liu, Chengyue Gong, and qiang liu. Flow straight and fast: Learning to generate and transfer data with rectified flow. In *The Eleventh International Conference on Learning Representations*, 2023. URL https://openreview.net/forum?id=XVjTT1nw5z.

Cheng Lu, Kaiwen Zheng, Fan Bao, Jianfei Chen, Chongxuan Li, and Jun Zhu. Maximum likelihood training for score-based diffusion odes by high order denoising score matching. In *International Conference on Machine Learning*, pp. 14429–14460. PMLR, 2022.

Cheng Lu, Huayu Chen, Jianfei Chen, Hang Su, Chongxuan Li, and Jun Zhu. Contrastive energy prediction for exact energy-guided diffusion sampling in offline reinforcement learning. In Andreas Krause, Emma Brunskill, Kyunghyun Cho, Barbara Engelhardt, Sivan Sabato, and Jonathan Scarlett (eds.), *Proceedings of the 40th International Conference on Machine Learning*, volume 202, pp. 22825–22855. PMLR, 5 2023. URL https://proceedings.mlr.press/v202/lu23d.html.

Gautam Mittal, Jesse Engel, Curtis Hawthorne, and Ian Simon. Symbolic music generation with diffusion models. *arXiv preprint arXiv:2103.16091*, 2021.

Kevin P Murphy. *Probabilistic machine learning: Advanced topics*. MIT press, 2023.

Alexander Quinn Nichol and Prafulla Dhariwal. Improved denoising diffusion probabilistic models. In Marina Meila and Tong Zhang (eds.), *Proceedings of the 38th International Conference on Machine Learning*, volume 139 of *Proceedings of Machine Learning Research*, pp. 8162–8171. PMLR, 18–24 Jul 2021. URL https://proceedings.mlr.press/v139/nichol21a.html.

Yazhe Niu, Jingxin Xu, Yuan Pu, Yunpeng Nie, Jinouwen Zhang, Shuai Hu, Liangxuan Zhao, Ming Zhang, and Yu Liu. Di-engine: A universal ai system/engine for decision intelligence. https://github.com/opendilab/DI-engine, 2021.

Xue Bin Peng, Aviral Kumar, Grace Zhang, and Sergey Levine. Advantage-weighted regression: Simple and scalable off-policy reinforcement learning, 2021. URL https://openreview.net/forum?id=ToWi1RjuEr8.

Jan Peters and Stefan Schaal. Reinforcement learning for operational space control. In *Proceedings 2007 IEEE International Conference on Robotics and Automation*, pp. 2111–2116, 2007. doi: 10.1109/ROBOT.2007.363633.

Jan Peters, Katharina Mulling, and Yasemin Altun. Relative entropy policy search. *Proceedings of the AAAI Conference on Artificial Intelligence*, 24(1):1607–1612, Jul. 2010. doi: 10.1609/aaai.v24i1.7727. URL https://ojs.aaai.org/index.php/AAAI/article/view/7727.

Michael Poli, Stefano Massaroli, Atsushi Yamashita, Hajime Asama, Jinkyoo Park, and Stefano Ermon. Torchdyn: implicit models and neural numerical methods in pytorch. In *Neural Information Processing Systems, Workshop on Physical Reasoning and Inductive Biases for the Real World*, volume 2, 2021.

Aram-Alexandre Pooladian, Heli Ben-Hamu, Carles Domingo-Enrich, Brandon Amos, Yaron Lipman, and Ricky T. Q. Chen. Multisample flow matching: Straightening flows with minibatch couplings. In Andreas Krause, Emma Brunskill, Kyunghyun Cho, Barbara Engelhardt, Sivan Sabato, and Jonathan Scarlett (eds.), *Proceedings of the 40th International Conference on Machine Learning*, volume 202 of *Proceedings of Machine Learning Research*, pp. 28100–28127. PMLR, 23–29 Jul 2023. URL https://proceedings.mlr.press/v202/pooladian23a.html.

Antonin Raffin, Ashley Hill, Adam Gleave, Anssi Kanervisto, Maximilian Ernestus, and Noah Dormann. Stable-baselines3: Reliable reinforcement learning implementations. *Journal of Machine Learning Research*, 22(268):1–8, 2021. URL http://jmlr.org/papers/v22/20-1364.html.

Allen Z Ren, Justin Lidard, Lars L Ankile, Anthony Simeonov, Pulkit Agrawal, Anirudha Majumdar, Benjamin Burchfiel, Hongkai Dai, and Max Simchowitz. Diffusion policy policy optimization. *arXiv preprint arXiv:2409.00588*, 2024.

Robin Rombach, Andreas Blattmann, Dominik Lorenz, Patrick Esser, and Björn Ommer. High-resolution image synthesis with latent diffusion models. In *Proceedings of the IEEE/CVF conference on computer vision and pattern recognition*, pp. 10684–10695, 2022.

Noah Y Siegel, Jost Tobias Springenberg, Felix Berkenkamp, Abbas Abdolmaleki, Michael Neunert, Thomas Lampe, Roland Hafner, Nicolas Heess, and Martin Riedmiller. Keep doing what worked: Behavioral modelling priors for offline reinforcement learning. *arXiv preprint arXiv:2002.08396*, 2020.

Jascha Sohl-Dickstein, Eric Weiss, Niru Maheswaranathan, and Surya Ganguli. Deep unsupervised learning using nonequilibrium thermodynamics. In Francis Bach and David Blei (eds.), *Proceedings of the 32nd International Conference on Machine Learning*, volume 37, pp. 2256–2265. PMLR, 5 2015. URL https://proceedings.mlr.press/v37/sohl-dickstein15.html.

Yang Song, Conor Durkan, Iain Murray, and Stefano Ermon. Maximum likelihood training of score-based diffusion models. In M Ranzato, A Beygelzimer, Y Dauphin, P S Liang, and J Wortman Vaughan (eds.), *Advances in Neural Information Processing Systems*, volume 34, pp. 1415–1428. Curran Associates, Inc., 2021a. URL https://proceedings.neurips.cc/paper_files/paper/2021/file/0a9fdbb17feb6ccb7ec405cfb85222c4-Paper.pdf.

Yang Song, Jascha Sohl-Dickstein, Diederik P Kingma, Abhishek Kumar, Stefano Ermon, and Ben Poole. Score-based generative modeling through stochastic differential equations. In *International Conference on Learning Representations*, 2021b. URL https://openreview.net/forum?id=PxTIG12RRHS.

Yuandong Tian, Qucheng Gong, Wenling Shang, Yuxin Wu, and C. Lawrence Zitnick. Elf: An extensive, lightweight and flexible research platform for real-time strategy games. *Advances in Neural Information Processing Systems (NIPS)*, 2017.

Alexander Tong, Nikolay Malkin, Kilian Fatras, Lazar Atanackovic, Yanlei Zhang, Guillaume Huguet, Guy Wolf, and Yoshua Bengio. Simulation-free schr "odinger bridges via score and flow matching, July 2023.

Alexander Tong, Kilian FATRAS, Nikolay Malkin, Guillaume Huguet, Yanlei Zhang, Jarrid Rector-Brooks, Guy Wolf, and Yoshua Bengio. Improving and generalizing flow-based generative models with minibatch optimal transport. *Transactions on Machine Learning Research*, 2024. ISSN 2835-8856. URL https://openreview.net/forum?id=CD9Snc73AW. Expert Certification.

Pascal Vincent. A connection between score matching and denoising autoencoders. *Neural Computation*, 23(7):1661–1674, 2011. doi: 10.1162/NECO_a_00142.

Patrick von Platen, Suraj Patil, Anton Lozhkov, Pedro Cuenca, Nathan Lambert, Kashif Rasul, Mishig Davaadorj, Dhruv Nair, Sayak Paul, William Berman, Yiyi Xu, Steven Liu, and Thomas Wolf. Diffusers: State-of-the-art diffusion models. https://github.com/huggingface/diffusers, 2022.

Zhendong Wang, Jonathan J Hunt, and Mingyuan Zhou. Diffusion policies as an expressive policy class for offline reinforcement learning. In *The Eleventh International Conference on Learning Representations*, 2023. URL https://openreview.net/forum?id=AHvFDPi-FA.

Jiayi Weng, Huayu Chen, Dong Yan, Kaichao You, Alexis Duburcq, Minghao Zhang, Yi Su, Hang Su, and Jun Zhu. Tianshou: A highly modularized deep reinforcement learning library. *Journal of Machine Learning Research*, 23(267):1–6, 2022. URL http://jmlr.org/papers/v23/21-1127.html.

Yifan Wu, George Tucker, and Ofir Nachum. Behavior regularized offline reinforcement learning, 2020. URL https://openreview.net/forum?id=BJg9hTNKPH.

Kaiwen Zheng, Cheng Lu, Jianfei Chen, and Jun Zhu. Improved techniques for maximum likelihood estimation for diffusion odes. In *International Conference on Machine Learning*, pp. 42363–42389. PMLR, 2023a.

Qinqing Zheng, Matt Le, Neta Shaul, Yaron Lipman, Aditya Grover, and Ricky TQ Chen. Guided flows for generative modeling and decision making. *arXiv preprint arXiv:2311.13443*, 2023b.

A Policy Optimization

We provide a detailed derivation of the forward KL and reverse KL divergence training objectives in Appendix A.1, and discuss the theoretical connections and differences between these objectives in Appendix A.2.

A.1 Derivation Details

The full derivation of the forward KL divergence training objective in Eq. 4 is as follows:

$$
\begin{aligned}
\mathcal{L}(\theta) &= \mathbb{E}_{s\sim\mathcal{D}}\left[D_{\mathrm{KL}}\left[\pi^*(\cdot|s)\|\pi_\theta(\cdot|s)\right]\right] \\
&= \mathbb{E}_{s\sim\mathcal{D}}\left[\int \pi^*(a|s)(\log\pi^*(a|s)-\log\pi_\theta(a|s))\mathrm{d}a\right] \\
&= \mathbb{E}_{s\sim\mathcal{D}}\left[\int \pi^*(a|s)\log\pi^*(a|s)\mathrm{d}a - \int \pi^*(a|s)\log\pi_\theta(a|s)\mathrm{d}a\right] \\
&= \mathbb{E}_{s\sim\mathcal{D}}\left[-\mathcal{H}_{\pi^*(a|s)} - \int \frac{e^{\beta(Q(s,a)-V(s))}}{Z(s)}\mu(a|s)\log\pi_\theta(a|s)\mathrm{d}a\right] \\
&= \mathbb{E}_{s\sim\mathcal{D},a\sim\mu(\cdot|s)}\left[-\frac{e^{\beta(Q(s,a)-V(s))}}{Z(s)}\log\pi_\theta(a|s)\right] - \mathbb{E}_{s\sim\mathcal{D}}\left[\mathcal{H}_{\pi^*(a|s)}\right] \\
&= \mathbb{E}_{s\sim\mathcal{D},a\sim\mu(\cdot|s)}\left[-\frac{e^{\beta(Q(s,a)-V(s))}}{Z(s)}\log\pi_\theta(a|s)\right] + C.
\end{aligned}
\tag{9}
$$

The full derivation of the reverse KL divergence training objective in Eq. 5 is as follows:

$$
\begin{aligned}
\mathcal{L}(\theta) &= \mathbb{E}_{s\sim\mathcal{D}}\left[D_{\mathrm{KL}}\left[\pi_\theta(\cdot|s)\|\pi^*(\cdot|s)\right]\right] \\
&= \mathbb{E}_{s\sim\mathcal{D}}\left[\int \pi_\theta(a|s)(\log\pi_\theta(a|s)-\log\pi^*(a|s))\mathrm{d}a\right] \\
&= \mathbb{E}_{s\sim\mathcal{D}}\left[\int \pi_\theta(a|s)(\log\pi_\theta(a|s)-\log(\frac{e^{\beta(Q(s,a)-V(s))}}{Z(s)}\mu(a|s)))\mathrm{d}a\right] \\
&= \mathbb{E}_{s\sim\mathcal{D}}\left[\int \pi_\theta(a|s)(\log\pi_\theta(a|s)-\log\mu(a|s)-\log(\frac{e^{\beta(Q(s,a)-V(s))}}{Z(s)}))\mathrm{d}a\right] \\
&= \mathbb{E}_{s\sim\mathcal{D}}\left[D_{\mathrm{KL}}\left[\pi_\theta(\cdot|s)\|\mu(\cdot|s)\right] + \int -\pi_\theta(a|s)\log(\frac{e^{\beta(Q(s,a)-V(s))}}{Z(s)})\mathrm{d}a\right] \\
&= \mathbb{E}_{s\sim\mathcal{D}}\left[D_{\mathrm{KL}}\left[\pi_\theta(\cdot|s)\|\mu(\cdot|s)\right] + \int -\pi_\theta(a|s)(\beta Q(s,a)-\beta V(s)-\log Z(s))\mathrm{d}a\right] \\
&= \mathbb{E}_{s\sim\mathcal{D}}\left[D_{\mathrm{KL}}\left[\pi_\theta(\cdot|s)\|\mu(\cdot|s)\right]\int \pi_\theta(a|s)\mathrm{d}a - \int \pi_\theta(a|s)\beta Q(s,a)\mathrm{d}a + (\beta V(s)+\log Z(s))\int \pi_\theta(a|s)\mathrm{d}a\right] \\
&= \mathbb{E}_{s\sim\mathcal{D}}\left[\int \pi_\theta(a|s)(-\beta Q(s,a)+D_{\mathrm{KL}}\left[\pi_\theta(\cdot|s)\|\mu(\cdot|s)\right])\mathrm{d}a + (\beta V(s)+\log Z(s))\int \pi_\theta(a|s)\mathrm{d}a\right] \\
&= \mathbb{E}_{s\sim\mathcal{D}}\left[\int \pi_\theta(a|s)(-\beta Q(s,a)+D_{\mathrm{KL}}\left[\pi_\theta(\cdot|s)\|\mu(\cdot|s)\right])\mathrm{d}a + \beta V(s)+\log Z(s)\right] \\
&= \mathbb{E}_{s\sim\mathcal{D}}\left[\int \pi_\theta(a|s)(-\beta Q(s,a)+D_{\mathrm{KL}}\left[\pi_\theta(\cdot|s)\|\mu(\cdot|s)\right])\mathrm{d}a\right] + \mathbb{E}_{s\sim\mathcal{D}}\left[\beta V(s)+\log Z(s)\right] \\
&= \mathbb{E}_{s\sim\mathcal{D},a\sim\pi_\theta(\cdot|s)}\left[-\beta Q(s,a)+D_{\mathrm{KL}}\left[\pi_\theta(\cdot|s)\|\mu(\cdot|s)\right]\right] + C.
\end{aligned}
\tag{10}
$$

A.2 Comparison Between Forward and Reverse KL Divergence Training Objectives

To obtain a neural network approximation $\pi_\theta(a|s)$ of the optimal policy

$$\pi^*(a|s) = \frac{e^{\beta(Q(s,a)-V(s))}}{Z(s)}\mu(a|s), \tag{11}$$

where the policy is a state-conditioned probability distribution, we can use either the forward KL divergence or reverse KL divergence as the training objective. Minimizing the KL divergence between $\pi_\theta(a|s)$ and the optimal policy $\pi^(a|s)$ reduces the discrepancy between the two distributions:

$$\text{Minimize} \quad D_{\text{KL}}\left[\pi^*(\cdot|s)\|\pi_\theta(\cdot|s)\right] \quad \text{or} \quad D_{\text{KL}}\left[\pi_\theta(\cdot|s)\|\pi^*(\cdot|s)\right]. \tag{12}$$

However, as is well-known in the literature (Murphy, 2023), the forward and reverse KL divergence objectives have different properties and implications. Training with the forward KL divergence tends to be *mode-covering*, preferring to cover all modes of the target distribution, including those with low probability mass. In contrast, training with the reverse KL divergence tends to be *mode-seeking*, concentrating on modes with high probability mass while potentially ignoring others.

Although we employ highly expressive probabilistic models, such as diffusion and flow models, which may mitigate these tendencies, the two training objectives still have different implications and may lead to different performance in practice. We provide a detailed term-by-term illustration of these two methods and their variants in Appendix A.2.1 and A.2.2, respectively.

A.2.1 Forward KL Divergence Training Objective

As shown in Eq. 13, the forward KL divergence training objective involves three components:

- The behavior policy $\mu(\cdot|s)$, from which actions are sampled.
- An exponential function of the advantage, $e^{\beta(Q(s,a)-V(s))}$, acting as an importance weight.
- The log-likelihood term $\log \pi_\theta(a|s)$ for maximum likelihood estimation (MLE).

$$\mathcal{L}(\theta) = \underbrace{\mathbb{E}_{s\sim\mathcal{D},a\sim\mu(\cdot|s)}}_{\text{Behavior Policy}}\left[-\underbrace{\frac{e^{\beta(Q(s,a)-V(s))}}{Z(s)}}_{\text{Advantage Weights}}\underbrace{\log \pi_\theta(a|s)}_{\text{MLE}}\right] + C. \tag{13}$$

In this objective, actions are sampled from the behavior policy $\mu(\cdot|s)$, which serves as a strong prior since it is static during optimization and pretrained to a well-established stage. Consequently, the range of actions evaluated is stable and rarely extends beyond the support of the behavior policy.

The exponential advantage term in Eq. 13 acts as an importance weight, emphasizing actions with higher advantage values. This term is crucial, as it focuses the learning on actions that improve policy performance. By weighting actions according to their advantages, suboptimal actions are filtered out in favor of optimal ones. If the advantage approaches zero for all actions, the objective simplifies to standard MLE.

In practice, some algorithms use explicit training objectives with advantage weights, such as QGPO (Lu et al., 2023) and GMPO, while others incorporate advantage weights during inference, such as SfBC (Chen et al., 2023) and IDQL (Hansen-Estruch et al., 2023), essentially making them sampling-based approaches when extracting optimal actions.

The MLE term $\log \pi_\theta(a|s)$ in Eq. 13 realizes the maximization of likelihood. However, as noted by Finlay et al. (2020), directly using the log-likelihood term for policy optimization with flow-based models can lead to ill-posed generative trajectories and poor performance. This is due to the infinite number of generation trajectories that can bridge two probability distributions, making the obtained trajectories sensitive.

Therefore, diffusion or flow models based on score matching or flow matching methods, which have static generation trajectories, are preferred over flow models trained by directly maximizing

log-likelihood. From a theoretical perspective, Song et al. (2021a) illustrated that conducting score matching with $\lambda(t) = g^2(t)$ is equivalent to training with an ELBO for maximizing likelihood estimation in diffusion models:

$$\mathcal{L}_{\text{MLE}}(\theta) = \mathbb{E}_{p(x)}\left[-\log p_\theta(x)\right] \leq \mathcal{L}_{\text{DSM}}(\theta) + C. \tag{14}$$

Recently, Lu et al. (2022) provided a more rigorous bound on how training diffusion models with score matching improves the log-likelihood, and Zheng et al. (2023a) presented similar proofs for flow matching methods. In general, any generative model training scheme that increases log-likelihood can serve as a substitute for $\log \pi_\theta$ in Eq. 13. Previous methods such as SfBC, IDQL, and QGPO use the score matching loss $\mathcal{L}_{\text{DSM}}(\theta)$, while in GMPO, we generalize this to include both the score matching loss $\mathcal{L}_{\text{DSM}}(\theta)$ and the flow matching loss $\mathcal{L}_{\text{CFM}}(\theta)$, collectively denoted as the matching loss $\mathcal{L}_{\text{Matching}}(\theta)$.

A.2.2 Reverse KL Divergence Training Objective

As shown in Eq. 15, the reverse KL divergence training objective comprises three components:

- The optimized policy $\pi_\theta(\cdot|s)$, from which actions are sampled.
- A value function $Q(s, a)$ that guides the policy optimization.
- A KL divergence term $D_{\text{KL}}(\pi_\theta(\cdot|s)|\mu(\cdot|s))$ acting as a proximal constraint.

$$\mathcal{L}(\theta) = \underbrace{\mathbb{E}_{s\sim\mathcal{D}, a\sim\pi_\theta(\cdot|s)}}_{\text{Optimized Policy}}\Bigg[\underbrace{-\beta Q(s,a)}_{\text{Guidance Function}} \underbrace{+ D_{\text{KL}}(\pi_\theta(\cdot|s)\|\mu(\cdot|s))}_{\text{Proximal Constraint}}\Bigg] + C. \tag{15}$$

In this objective, actions are sampled from the policy being optimized, $\pi_\theta(\cdot|s)$, which is initialized to the behavior policy $\mu(\cdot|s)$ but gradually diverges from it as optimization progresses guided by the value function. The value function $Q(s, a)$ provides guidance by emphasizing actions with higher values, encouraging the policy to focus on optimal actions, even if they are rare in the behavior policy. This contrasts with the forward KL objective, where actions are sampled from the behavior policy.

The proximal constraint term $D_{\text{KL}}(\pi_\theta(\cdot|s)|\mu(\cdot|s))$ enforces closeness to the behavior policy to prevent drastic updates that may degrade performance. While GMPG retains this KL divergence term, other algorithms replace it with alternative regularization methods, such as the score matching loss in Diffusion-QL (Wang et al., 2023) or a score regularization term in SRPO (Chen et al., 2024).

B Generative Models

Generative models generate samples from a target distribution $p(x)$, or $p(x|c)$ when conditioned on context c. This work focuses on two types of continuous-time generative models: diffusion models and flow models.

B.1 Diffusion Models

Diffusion models use a forward diffusion process to train the score function and a reverse diffusion process for sampling. Given a fixed data or target distribution, a diffusion model is determined by the diffusion process path. A common path, governed by a linear stochastic differential equation (SDE), is:

$$\mathrm{d}x = f(t)x_t\mathrm{d}t + g(t)\mathrm{d}w_t. \tag{16}$$

The transition distribution of a point $x \in \mathbb{R}^d$ from time 0 to t is:

$$p(x_t|x_0) \sim \mathcal{N}(x_t|\alpha_t x_0, \sigma_t^2 I). \tag{17}$$

The drift coefficient $f(t)$ and diffusion coefficient $g(t)$ are related to the noise level σ_t and scale level α_t:

$$f(t) = \frac{\mathrm{d}\log\alpha_t}{\mathrm{d}t}, \tag{18}$$

$$g^2(t) = \frac{\mathrm{d}\sigma_t^2}{\mathrm{d}t} - 2\frac{\mathrm{d}\log\alpha_t}{\mathrm{d}t}\sigma_t^2. \tag{19}$$

The drift and diffusion coefficients for Linear Variance-Preserving SDE (VP-SDE) model (Song et al., 2021b) and Generalized VP-SDE (GVP) model (Albergo & Vanden-Eijnden, 2023) are defined as:

$$\begin{aligned} \text{VP-SDE:} \quad & \alpha_t = \exp\left(-\frac{1}{2}\int_0^t \beta_s \,\mathrm{d}s\right), && \sigma_t = \sqrt{1 - \exp\left(-\int_0^t \beta_s \,\mathrm{d}s\right)}. \\ \text{GVP:} \quad & \alpha_t = \cos\left(\frac{1}{2}\pi t\right), && \sigma_t = \sin\left(\frac{1}{2}\pi t\right). \end{aligned} \tag{20}$$

Here, β_t follows the same scaling as in Song et al. (2021b).

The reverse process of the diffusion model is derived from the Fokker-Planck equation and can be expressed as an ODE:

$$\frac{\mathrm{d}x_t}{\mathrm{d}t} = v(x_t) = f(t)x_t - \frac{1}{2}g^2(t)\nabla_{x_t}\log p(x_t), \tag{21}$$

where $v(x_t)$ is the velocity function and $\nabla_{x_t}\log p(x_t)$ is the score function, typically modeled by a neural network with parameters θ, denoted as $v_\theta(x_t)$ and $s_\theta(x_t)$, respectively.

Training the diffusion model involves a matching objective $\mathcal{L}_{\text{Matching}}(\theta)$, which can utilize either the Score Matching method by Hyvärinen (2005) or the Flow Matching method by Lipman et al. (2023). The Score Matching objective is defined as a weighted Mean Squared Error (MSE) loss between the score function model and the gradient of the log density of the target distribution:

$$\mathcal{L}_{\text{SM}} = \frac{1}{2}\int_0^1 \mathbb{E}_{p(x_t)}\left[\lambda(t)\|s_\theta(x_t) - \nabla_{x_t}\log p(x_t)\|^2\right]\mathrm{d}t. \tag{22}$$

In practice, the Denoising Score Matching loss $\mathcal{L}_{\text{DSM}}$ is used for every diffusion path conditioned on x_0 because it shares the same gradient, $\nabla\mathcal{L}_{\text{DSM}} = \nabla\mathcal{L}_{\text{SM}}$, as shown by Vincent (2011):

$$\mathcal{L}_{\text{DSM}} = \frac{1}{2}\int_0^1 \mathbb{E}_{p(x_t,x_0)}\left[\lambda(t)\|s_\theta(x_t) - \nabla_{x_t}\log p(x_t|x_0)\|^2\right]\mathrm{d}t. \tag{23}$$

We can use both Vanilla Score Matching proposed by Ho et al. (2020) and Maximum Likelihood Score Matching by Song et al. (2021a). These methods differ in the weighting of the score matching loss:

$$\begin{aligned} \text{Vanilla Score Matching:} \quad & \lambda_{\text{SM}}(t) = \sigma_t^2. \\ \text{Maximum Likelihood Score Matching:} \quad & \lambda_{\text{MLSM}}(t) = g^2(t). \end{aligned} \tag{24}$$

The Flow Matching method uses a weighted Mean Squared Error (MSE) loss between the velocity function of the reverse diffusion process and a target velocity:

$$\mathcal{L}_{\text{FM}} = \frac{1}{2}\int_0^1 \mathbb{E}_{p(x_t)}\left[\|v_\theta(x_t) - v(x_t)\|^2\right]\mathrm{d}t. \tag{25}$$

In practice, a Conditional Flow Matching loss $\mathcal{L}_{\text{CFM}}$ for every flow path conditioned on x_0 and x_1 is used, as it shares the same gradient, $\nabla\mathcal{L}_{\text{CFM}} = \nabla\mathcal{L}_{\text{FM}}$, as shown by Lipman et al. (2023) and Tong et al. (2024):

$$\mathcal{L}_{\text{CFM}} = \frac{1}{2}\int_0^1 \mathbb{E}_{p(x_t,x_0,x_1)}\left[\|v_\theta(x_t) - v(x_t|x_0,x_1)\|^2\right]\mathrm{d}t. \tag{26}$$

We use both the Score Matching loss $\mathcal{L}_{\text{DSM}}$ and the Flow Matching loss $\mathcal{L}_{\text{CFM}}$ to train the diffusion models.

B.2 FLOW MODELS

Continuous normalizing flows (CNFs), introduced by Chen et al. (2018) and Grathwohl et al. (2019), are the first continuous-time generative models capable of modeling complex target distributions. However, their simulation-based maximum likelihood training process is unstable, often resulting in poor performance and distorted generative paths, as illustrated by Finlay et al. (2020).

To address these issues, recent works (Lipman et al. (2023); Liu et al. (2023); Pooladian et al. (2023); Albergo & Vanden-Eijnden (2023); Tong et al. (2024)) propose CNFs with simulation-free objectives, similar to diffusion models that use designed and fixed diffusion paths as regression objectives. These approaches are more stable during training and retain the advantage that the source distribution can be arbitrary, unlike diffusion models which require a Gaussian source distribution.

For the flow models I-CFM (Tong et al., 2024) investigated in this paper, the flow path is defined as:

$$p(x_t|x_0, x_1) = \mathcal{N}(x_t|tx_1 + (1-t)x_0, \sigma^2 I). \tag{27}$$

The velocity function is given by:

$$v(x_t|x_0, x_1) = x_1 - x_0. \tag{28}$$

The flow model $v_\theta(x_t)$ is trained using the Conditional Flow Matching loss $\mathcal{L}_{\text{CFM}}$.

C GENERATIVE POLICIES

As shown in Table 2, generative policy training schemes can be categorized based on their use of either the forward KL divergence (Eq. 4) or the reverse KL divergence (Eq. 5). SfBC and QGPO use forward KL divergence, while Diffusion-QL and SRPO employ reverse KL divergence. IDQL also uses forward KL divergence but differs slightly due to its unique importance weighting for sampling.

C.1 SFBC: SELECTING FROM BEHAVIOR CANDIDATES

SfBC (Chen et al., 2023) trains a diffusion model as the behavior policy using the score matching loss (Eq. 2) and trains the Q-function model with an In-Support Q-Learning method (Eq. 29):

$$\mathcal{L}_{\text{in-support QL}}(\xi) = \mathbb{E}_{(s,a,s')\sim\mathcal{D}, a'_i\sim\mu}\left[\left(Q_\xi(s,a) - r(s,a) - \gamma\left[\frac{\sum_{i=1}^N e^{Q_\xi(s',a'_i)} Q_\xi(s',a'_i)}{\sum_{i=1}^N e^{Q_\xi(s',a'_i)}}\right]\right)^2\right]. \tag{29}$$

Actions are sampled by selecting the one with the highest Q-value among N candidates generated by the behavior policy.

C.2 QGPO: Q-GUIDED POLICY OPTIMIZATION

QGPO (Lu et al., 2023) enhances SfBC by distilling the Q-function into an intermediate energy guidance model, $\mathcal{E}_\phi(s, a, t)$, using the Contrastive Energy Prediction (CEP) method:

$$\mathcal{L}_{\text{CEP}}(\phi) = -\mathbb{E}_{t,(s,a)\sim\mathcal{D}, a_i\sim\mu}\left[\sum_{i=1}^N \frac{e^{\beta Q(s,a_i)}}{\sum_{i=1}^N e^{\beta Q(s,a_i)}} \log \frac{e^{\mathcal{E}_\phi(s,a_i,t)}}{\sum_{i=1}^N e^{\mathcal{E}_\phi(s,a_i,t)}}\right]. \tag{30}$$

This approach allows the optimal policy to be sampled using a combination of the score functions of the behavior policy and the energy guidance model:

$$\nabla_{a_t}\pi(a_t|s_t) = \nabla_{a_t}\log\mu(a_t|s_t) + \nabla_{a_t}\mathcal{E}_\phi(s_t, a_t, t). \tag{31}$$

However, this method is not suitable for flow models, as their score functions cannot be easily obtained.

C.3 IDQL: IMPLICIT DIFFUSION Q-LEARNING

IDQL (Hansen-Estruch et al., 2023) employs Implicit Q-Learning as described in Eq. 32:

$$\begin{aligned}
\mathcal{L}_{\text{IQL-}V}(\psi) &= \mathbb{E}_{(s,a)\sim\mathcal{D}}\left[\mathcal{L}_2^\tau\left(Q_\xi(s,a) - V_\psi(s)\right)\right] \\
\mathcal{L}_2^\tau(u) &= |\tau - \mathbb{1}(u \le 0)|u^2 \\
\mathcal{L}_{\text{IQL-}Q}(\xi) &= \mathbb{E}_{(s,a)\sim\mathcal{D}}\left[\left(Q_\xi(s,a) - r(s,a) - V_\psi(s')\right)^2\right].
\end{aligned} \tag{32}$$

IDQL implicitly constructs an optimal policy model through importance sampling based on the Q-values of action candidates. A batch of backup actions is sampled from a behavior policy, and the optimal action is selected through inference using the Q-function model.

Hansen-Estruch et al. (2023) demonstrated that if an implicit actor satisfies the following equation:

$$V^*(s) = \mathbb{E}_{a\sim\pi_{\text{implicit}}(a|s)}[Q^*(s,a)], \tag{33}$$

for an optimal Q-function and value function in IQL, then the implicit actor is given by:

$$\pi_{\text{implicit}}(a|s) \propto \frac{\left|\frac{\partial}{\partial V(s)}(Q(s,a)-V^*(s))\right|}{|Q(s,a)-V^*(s)|}\mu(a|s). \tag{34}$$

where $\frac{\left|\frac{\partial}{\partial V(s)}(Q(s,a)-V^*(s))\right|}{|Q(s,a)-V^*(s)|}$ is the importance weight for action a in state s.

C.4 SRPO: Score-based Regularized Policy Optimization

SRPO (Chen et al., 2024) pretrains a behavior policy using a diffusion model with a score matching loss, as described in Eq. 2. The Q-function model is then independently trained using the IQL method outlined in Eq. 32.

The Dirac or Gaussian policy is trained by distilling guidance from the Q-function model, using the score function of the behavior policy as a regularizer to prevent significant divergence:

$$\mathcal{L}_{\text{SRPO}}(\psi) = -\beta Q(s,a) + w(t)(\epsilon_\psi(a_t|s) - \epsilon). \tag{35}$$

C.5 Diffusion-QL

Diffusion-QL (Wang et al., 2023) trains the Q-function model using the conventional Bellman operator with the double Q-learning trick:

$$\mathcal{L}_{\text{Diffusion-QL}}(\xi) = \mathbb{E}_{(s,a,s')\sim\mathcal{D},a'\sim\pi}\left[\left(Q_\xi(s,a) - r(s,a) - \gamma \min_{i=1,2} Q_{\xi_i}(s',a')\right)^2\right]. \tag{36}$$

Next, Q-value function guidance is incorporated into the policy using the following training objective:

$$\mathcal{L}_{\text{Diffusion-QL}}(\theta) = \mathbb{E}_{s\sim\mathcal{D},a\sim\pi_\theta(\cdot|s)}\left[-\beta Q(s,a) + \mathcal{L}_{\text{DSM}}(\theta)\right], \tag{37}$$

where $\mathcal{L}_{\text{DSM}}(\theta)$ is the score matching loss for the diffusion model, as defined in Eq. 2.

During inference, the authors adopt a resampling strategy similar to Implicit Diffusion Q-Learning, where the action with the highest Q-value is selected using a softmax function among 50 candidates. A small performance drop is observed in Diffusion-QL when the resampling strategy is disabled, indicating that the policy model relies on the Q-function model to achieve optimal performance.

C.6 GMPO: Generative Model Policy Optimization

The derivation of Eq. 6 is:

$$\begin{aligned}
\mathcal{L}_{\text{GMPO}}(\theta) &= \mathbb{E}_{s\sim\mathcal{D},a\sim\pi^*(\cdot|s)}\left[\mathcal{L}_{\text{Matching}}(\theta)\right] \\
&= \mathbb{E}_{s\sim\mathcal{D}}\left[\int \pi^*(a|s)\mathcal{L}_{\text{Matching}}(\theta)\mathrm{d}a\right] \\
&= \mathbb{E}_{s\sim\mathcal{D}}\left[\int \frac{e^{\beta(Q(s,a)-V(s))}}{Z(s)}\mu(a|s)\mathcal{L}_{\text{Matching}}(\theta)\mathrm{d}a\right] \\
&= \mathbb{E}_{s\sim\mathcal{D}}\left[\int \mu(a|s)\frac{e^{\beta(Q(s,a)-V(s))}}{Z(s)}\mathcal{L}_{\text{Matching}}(\theta)\mathrm{d}a\right] \\
&= \mathbb{E}_{s\sim\mathcal{D},a\sim\mu(\cdot|s)}\left[\frac{e^{\beta(Q(s,a)-V(s))}}{Z(s)}\mathcal{L}_{\text{Matching}}(\theta)\right].
\end{aligned} \tag{38}$$

We present the GMPO algorithm in Algorithm 1.

Algorithm 1 Generative Model Policy Optimization (GMPO)

Initialize π_θ, Q_ξ, V_ϕ.
// Critic training (Implicit Q-Learning)
for epoch = 1 to N **do**
  $\phi \leftarrow \phi - \lambda_Q \nabla_\phi L_V$ (Eq. 32)
  $\xi \leftarrow \xi - \lambda_V \nabla_\xi L_Q$ (Eq. 32)
// Policy training (Advantage-Weighted Regression)
for epoch = 1 to N **do**
  $\theta \leftarrow \theta - \lambda_\pi \nabla_\theta L_\pi$ (Eq. 7)

For the score matching objective, the GMPO loss is defined as:

$$\mathcal{L}_{\text{GMPO-SM}}(\theta) = -\mathbb{E}_{s\sim\mathcal{D},a\sim\mu(\cdot|s)}\left[\frac{e^{\beta(Q(s,a)-V(s))}}{Z(s)}\mathbb{E}_{p(a_t|a)}\left[\frac{1}{2}\lambda(t)\|s_\theta(a_t|s) - \nabla_{a_t}\log p(a_t|a,s)\|^2\right]\right]. \tag{39}$$

For the flow matching objective, the GMPO loss is defined as:

$$\mathcal{L}_{\text{GMPO-FM}}(\theta) = -\mathbb{E}_{s\sim\mathcal{D},a\sim\mu(\cdot|s)}\left[\frac{e^{\beta(Q(s,a)-V(s))}}{Z(s)}\mathbb{E}_{p(a_t|a)}\left[\frac{1}{2}\|v_\theta(a_t|s) - v(a_t|a,s)\|^2\right]\right]. \tag{40}$$

To address potential numerical issues with the importance sampling weight in exponential form, we can clamp the weight if it becomes too large. This adjustment reduces the emphasis on high Q-value actions but does not significantly impact performance.

Alternatively, if clamping the weight is not desired, using a softmax function to approximate the importance weight can also circumvent numerical issues. This approach is similar to QGPO and is formulated as:

$$\mathcal{L}_{\text{GMPO-Softmax}}(\theta) = -\mathbb{E}_{s\sim\mathcal{D},a_{1:K}\sim\mu(\cdot|s)}\left[\frac{e^{\beta Q(s,a_i)}}{\sum_{j=1}^K e^{\beta Q(s,a_j)}}\mathcal{L}_{\text{Matching}}(\theta)\right]. \tag{41}$$

However, this requires sampling K actions from the behavior policy, increasing computational cost during training.

We present the GMPO algorithm with the behavior policy in Algorithm 2.

Algorithm 2 Generative Model Policy Optimization (GMPO) with Behavior Policy

Initialize μ_{θ_1}, π_{θ_2}, Q_ξ, V_ϕ.
// Behavior Policy Pretraining (Score Matching or Flow Matching)
for epoch = 1 to N **do**
  $\theta_1 \leftarrow \theta_1 - \lambda_\mu \nabla_{\theta_1} L_\mu$ (Eq. 2 or Eq. 3)
// Critic Training (Implicit Q-Learning)
for epoch = 1 to N **do**
  $\phi \leftarrow \phi - \lambda_Q \nabla_\phi L_V$ (Eq. 32)
  $\xi \leftarrow \xi - \lambda_V \nabla_\xi L_Q$ (Eq. 32)
// Policy Training (Advantage-Weighted Regression)
for epoch = 1 to N **do**
  Sample $a_i \sim \mu_{\theta_1}$
  $\theta_2 \leftarrow \theta_2 - \lambda_\pi \nabla_{\theta_2} L_\pi$ (Eq. 41)

C.7 GMPG: Generative Model Policy Gradient

We present the GMPG algorithm in Algorithm 3.

Algorithm 3 Generative Model Policy Gradient (GMPG)

Initialize μ_{θ_1}, π_{θ_2}, Q_ξ, V_ϕ.
// Behavior Policy Pretraining (Flow Matching)
for epoch = 1 to N **do**
  $\theta_1 \leftarrow \theta_1 - \lambda_\mu \nabla_{\theta_1} L_\mu$ (Eq. 3)
// Critic Training (Implicit Q-Learning)
for epoch = 1 to N **do**
  $\phi \leftarrow \phi - \lambda_Q \nabla_\phi L_V$ (Eq. 32)
  $\xi \leftarrow \xi - \lambda_V \nabla_\xi L_Q$ (Eq. 32)
// Policy Training (Policy Gradient)
$\theta_2 \leftarrow \theta_1$
for epoch = 1 to N **do**
  $\theta_2 \leftarrow \theta_2 - \lambda_\pi \nabla_{\theta_2} L_\pi$ (Eq. 8 or Eq. 42)

Since the vanilla GMPG loss relies on sampling from a dynamic generative model, policy training can become unstable with a small batch size, particularly when the optimized policy encounters state-action spaces with scarce data.

To stabilize the training process, we can use an importance sampling weight by sampling from a static generative model, which in practice is the behavior policy $\mu(\cdot|s)$:

$$\nabla_\theta \mathcal{L}_{\text{GMPG-Static}}(\theta) =$$
$$\mathbb{E}_{s\sim\mathcal{D},a\sim\mu(\cdot|s)}\left[\frac{e^{\beta(Q(s,a)-V(s))}}{Z(s)}(-\beta Q(s,a)+\log\pi_\theta(a|s)-\log\mu(a|s))\nabla_\theta\log\pi_\theta(a|s)\right]$$
$$\mathbb{E}_{s\sim\mathcal{D},a_{1:K}\sim\mu(\cdot|s)}\left[\frac{e^{\beta Q(s,a_i)}}{\sum_{j=1}^K e^{\beta Q(s,a_j)}}(-\beta Q(s,a_i)+\log\pi_\theta(a_i|s)-\log\mu(a_i|s))\nabla_\theta\log\pi_\theta(a_i|s)\right]. \tag{42}$$

It is important to note that GMPG works well only when the generative model's neural network output is a velocity function v_θ. Training encounters numerical issues when using a noise function ϵ_θ as the neural network output. If using a neural network as the noise function, converting it to a velocity function by Eq 21:

$$v_\theta(x_t) = f(t)x_t - \frac{1}{2}g^2(t)\nabla_{x_t}\log p_\theta(x_t) = f(t)x_t - \frac{g^2(t)}{2\sigma(t)}\epsilon_\theta(x_t). \tag{43}$$

As $g^2(t)$ approaches 0 when sampling from $t=1$ to $t=0$, $\sigma(t)$ approching 0 much faster than $g^2(t)$. Therefore, since the noise function ϵ_θ is a neural network output and is in the range $[-D, D]$, the velocity can become unstable. Although this is not a major issue during sampling $\mathrm{d}x = v\mathrm{d}t$, since $\mathrm{d}t$ is not 0 for ODE solvers, it can cause numerical instability during training if using neural ODE implementation for backward gradient computation. Therefore, we use only the velocity model for GMPG experiments across different generative models.

C.7.1 Calculation of Probability Density

The calculation of $\log p(x)$ is crucial for training the generative model via the GMPG algorithm, following the approach of Chen et al. (2018); Grathwohl et al. (2019). Since sampling through the generative model involves solving an ODE defined by Eq. 21, the probability density of the sampled variable x_t can be computed using the instantaneous change of variables theorem:

$$\begin{bmatrix} x_0 \\ \log p(x_0) - \log p(x_1) \end{bmatrix} = \int_{t_1}^{t_0} \begin{bmatrix} v_\theta(x(t),t) \\ -\mathrm{Tr}\left(\frac{\partial v_\theta}{\partial x(t)}\right) \end{bmatrix} \mathrm{d}t. \tag{44}$$

Here, $x_1 \sim \mathcal{N}(0, I)$ and $\log p(x_1)$ is tractable. Thus, $\log p(x_0)$ can be obtained by integrating from $t_1 = 1$ to $t_0 = 0$.

To reduce the computational cost of calculating the trace of the Jacobian matrix, we use Hutchinson's trace estimator (Hutchinson, 1990), which approximates the trace as:

$$\text{Tr}\left(\frac{\partial v_\theta}{\partial x(t)}\right) \approx \mathbb{E}_{\epsilon\sim\mathcal{N}(0,I)}\left[\epsilon^\top \frac{\partial v_\theta}{\partial x(t)}\epsilon\right], \tag{45}$$

where $\epsilon \sim \mathcal{N}(0, I)$ is a random vector sampled from a standard Gaussian distribution.

C.8 2D Toy Example

To visually illustrate the fundamental differences between the proposed generative policies, we use a simple 2D toy example with the Swiss Roll dataset. We designed a value function for this dataset, where the value changes from -3.5 to 1.5 as the spiral extends outward (see Figure 2).

We evaluate the generation trajectories of models trained with GMPO and GMPG on this example, with results shown in Figure 3. This demonstration highlights that GMPO and GMPG operate differently: GMPO filters data points and learns the path to these points, whereas GMPG attempts to keep the generation path within the manifold of the original data distribution. Consequently, the Swiss Roll shape is largely preserved in GMPG trajectories but not in GMPO trajectories.

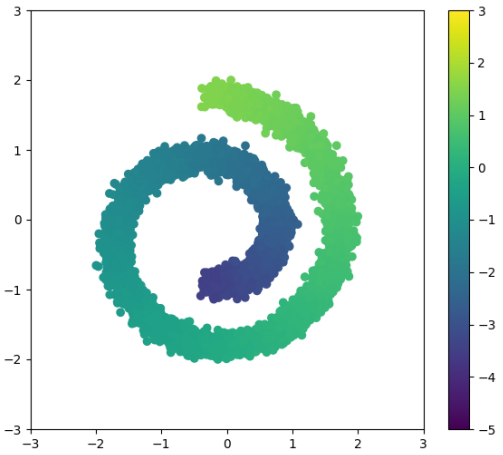

Figure 2: 2D toy Swiss Roll dataset with assigned value function. Values range from -3.5 to 1.5 as the spiral extends outward. Colors represent data point values. A small noise $\epsilon = 0.6$ is added for better visualization.

D Experiments

D.1 Training details

Training is conducted on an NVIDIA A100 GPU with 80GB of memory. The duration for each experiment ranges from 24 to 72 hours, depending on the model complexity, dataset size, and chosen training steps. Table 7 lists the hyperparameters used for training generative models and reinforcement learning models.

We tune the temperature coefficient β for different tasks, as it affects the strength of the Q-value guidance. Choosing the appropriate value is sometimes essential for optimal policy model performance, as shown in Table 8.

Table 7: Hyper-parameters for training generative models and reinforcement learning models

Training	
Optimizer	Adam
τ in IQL	0.7
τ in IQL for AntMaze	0.9
Discount factor γ	0.99
Learning rate for pretraining behavior model	10^{-4}
Learning rate for critic training	10^{-4}
Learning rate for policy extraction	10^{-4}
Learning rate for policy extraction (special cases)	$10^{-5} \sim 10^{-6}$
Batchsize for pretraining behavior model	4096
Batchsize for critic training	4096
Batchsize for policy extraction in GMPO	4096
Batchsize for policy extraction in GMPG	40960
Sampling steps T	1000
Evaluation	
Solver for ODE	Euler-Maruyama
Sampling steps T	32

Table 8: Temperature coefficient β value tuning over different tasks

Task	GMPO	GMPG
D4RL Locomotion		
halfcheetah-medium-expert-v2	1.0	4.0
hopper-medium-expert-v2	1.0	4.0
walker2d-medium-expert-v2	1.0	4.0
halfcheetah-medium-v2	1.0	1.0
hopper-medium-v2	16.0	20.0
walker2d-medium-v2	8.0	1.0
halfcheetah-medium-replay-v2	4.0	4.0
hopper-medium-replay-v2	6.0	8.0
walker2d-medium-replay-v2	8.0	4.0
D4RL AntMaze		
antmaze-umaze-v0	8.0	1.0
antmaze-umaze-diverse-v0	16.0	1.0
antmaze-medium-play-v0	12.0	0.25
antmaze-medium-diverse-v0	12.0	0.25
antmaze-large-play-v0	16.0	0.5
antmaze-large-diverse-v0	4.0	1.0
RL Unplugged DeepMind Control Suite		
Cartpole swingup	1.0	4.0
Cheetah run	1.0	4.0
Humanoid run	1.0	4.0
Manipulator insert ball	1.0	4.0
Walker stand	1.0	4.0
Finger turn hard	1.0	4.0
Fish swim	1.0	4.0
Manipulator insert peg	1.0	4.0
Walker walk	1.0	4.0

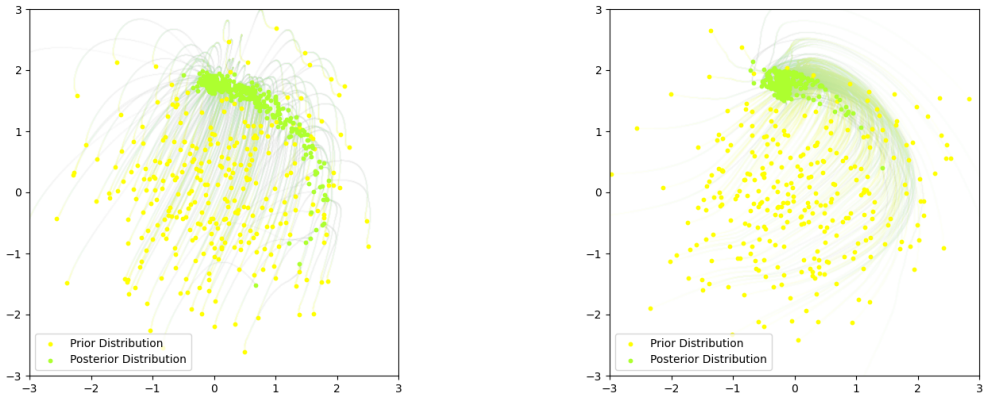

(a) GMPO (b) GMPG

Figure 3: Generation trajectories of models trained by GMPO and GMPG on the 2D toy Swiss Roll dataset. Colors indicate time stamps of data points during generation.

Table 9: Performance comparison of on D4RL datasets across QGPO, SRPO and IDQL algorithms between GenerativeRL and original papers.

	Original Papers			**GenerativeRL**		
Algo. type	**QGPO**	**IDQL**	**SRPO**	**QGPO**	**IDQL**	**SRPO**
Model type	**VPSDE**	**DDPM**	**VPSDE**	**VPSDE**	**VPSDE**	**VPSDE**
Function type	$\epsilon(x_t, t)$	$\epsilon(x_t, t)$	$\epsilon(x_t, t)$	$\epsilon(x_t, t)$	$\epsilon(x_t, t)$	$\epsilon(x_t, t)$
Pretrain scheme	Eq. 2	Eq. 2	Eq. 2	Eq. 2	Eq. 2	Eq. 2
Finetune scheme	Eq. 30	/	Eq. 35	Eq. 30	/	Eq. 35
halfcheetah-medium-expert-v2	93.5	95.9	92.2	92.0 ± 1.5	91.7 ± 2.4	86.7 ± 3.7
hopper-medium-expert-v2	108.0	108.6	100.1	107.0 ± 0.9	96.8 ± 10.4	100.8 ± 9.3
walker2d-medium-expert-v2	110.7	112.7	114.0	107.3 ± 1.3	107.0 ± 0.5	118.7 ± 1.4
halfcheetah-medium-v2	54.1	51.0	60.4	44.0 ± 0.7	43.7 ± 2.8	51.4 ± 2.9
hopper-medium-v2	98.0	65.4	95.5	80.1 ± 7.0	72.1 ± 17.6	97.2 ± 3.3
walker2d-medium-v2	86.0	82.5	84.4	82.8 ± 2.7	82.0 ± 2.4	85.6 ± 2.1
halfcheetah-medium-replay-v2	47.6	45.9	51.4	42.5 ± 1.7	41.6 ± 8.4	47.2 ± 4.5
hopper-medium-replay-v2	96.9	92.1	101.2	99.3 ± 1.8	89.1 ± 3.1	78.2 ± 12.1
walker2d-medium-replay-v2	84.4	85.1	84.6	81.1 ± 4.2	80.4 ± 9.2	79.6 ± 7.6
Average (Locomotion)	86.6	82.1	87.1	81.8 ± 2.4	78.3 ± 6.3	82.8 ± 5.1

D.2 More experiments

We provide comparative performance scores for the QGPO, SRPO, and IDQL algorithms on D4RL datasets, using both our implementation and the scores reported in the original papers, as shown in Table 9.

We conduct experiments on the D4RL to evaluate the performance of generative policy using different generative models as shown in Table 10.

We conducted additional experiments on the D4RL AntMaze datasets to evaluate the performance of GMPO and GMPG, as shown in Table 11. In this 2D maze environment, the agent navigates to a goal location, with a larger action and state space compared to previous D4RL locomotion experiments. Performance is evaluated based on the average return over 100 episodes. Our results indicate that the proposed generative policies, GMPO and GMPG, achieve competitive performance compared to the baselines.

Table 10: Performance comparison of on D4RL datasets over different generative models over GMPO and GMPG.

Algo. type	**GMPO**			**GMPG**		
Model type	**VPSDE**	**GVP**	**I-CFM**	**VPSDE**	**GVP**	**I-CFM**
Function type	$\epsilon(x_t, t)$	$v(x_t, t)$	$v(x_t, t)$	$v(x_t, t)$	$v(x_t, t)$	$v(x_t, t)$
Pretrain scheme	/	/	/	Eq. 3	Eq. 3	Eq. 3
Fintune scheme	Eq. 39	Eq. 40	Eq. 40	Eq. 8	Eq. 8	Eq. 8
halfcheetah-medium-expert-v2	91.8 ± 3.3	91.9 ± 3.2	83.3 ± 3.7	89.0 ± 6.4	84.2 ± 8.0	86.9 ± 4.5
hopper-medium-expert-v2	111.1 ± 1.34	112.0 ± 1.8	87.4 ± 25.7	107.8 ± 1.9	101.6 ± 2.9	101.7 ± 1.4
walker2d-medium-expert-v2	107.7 ± 0.4	108.1 ± 0.7	110.3 ± 0.7	112.8 ± 1.2	110.0 ± 1.2	110.7 ± 0.3
halfcheetah-medium-v2	49.8 ± 2.6	49.9 ± 2.7	48.0 ± 2.9	57.0 ± 3.1	46.0 ± 2.7	51.4 ± 2.9
hopper-medium-v2	71.9 ± 22.1	74.6 ± 21.2	69.5 ± 20.4	101.1 ± 2.6	100.1 ± 1.6	92.8 ± 18.1
walker2d-medium-v2	79.0 ± 13.2	81.1 ± 4.3	79.2 ± 7.6	91.9 ± 0.9	92.0 ± 1.1	82.6 ± 2.3
halfcheetah-medium-replay-v2	36.6 ± 2.4	42.3 ± 3.6	41.7 ± 3.2	50.5 ± 2.7	39.1 ± 5.4	41.0 ± 3.5
hopper-medium-replay-v2	89.2 ± 7.4	97.8 ± 3.8	86.0 ± 2.6	86.3 ± 10.5	103.4 ± 2.1	104.2 ± 2.0
walker2d-medium-replay-v2	84.5 ± 4.6	86.4 ± 1.7	80.9 ± 5.3	90.1 ± 2.2	81.7 ± 3.2	79.4 ± 3.2
Average (Locomotion)	80.2 ± 4.2	82.7 ± 4.8	76.2 ± 8.0	87.3 ± 3.5	84.2 ± 3.2	83.4 ± 4.2

Table 11: Performance evaluation on D4RL AntMaze of different generative policies.

Environment	**SfBC**	**Diffusion-QL**	**QGPO**	**IDQL**	**SRPO**	**GMPO**	**GMPG**
Model type	**VPSDE**	**DDPM**	**VPSDE**	**DDPM**	**VPSDE**	**GVP**	**VPSDE**
Function type	$\epsilon(x_t, t)$	$\epsilon(x_t, t)$	$\epsilon(x_t, t)$	$\epsilon(x_t, t)$	$\epsilon(x_t, t)$	$v(x_t, t)$	$v(x_t, t)$
Pretrain scheme	Eq. 2	Eq. 2	Eq. 2	Eq. 2	Eq. 2	/	Eq. 3
Fintune scheme	/	Eq. 37	Eq. 30	/	Eq. 35	Eq. 40	Eq. 8
antmaze-umaze-v0	92.0	93.4	96.4	94.0	97.1	94.2 ± 0.9	92.5 ± 1.6
antmaze-umaze-diverse-v0	85.3	66.2	74.4	80.2	82.1	76.8 ± 11.2	76.0 ± 3.4
antmaze-medium-play-v0	81.3	76.6	83.6	84.5	80.7	84.6 ± 4.2	62.5 ± 3.7
antmaze-medium-diverse-v0	82.0	78.6	83.8	84.8	75.0	69.0 ± 5.6	67.2 ± 2.0
antmaze-large-play-v0	59.3	46.4	66.6	63.5	53.6	49.2 ± 11.2	40.1 ± 8.6
antmaze-large-diverse-v0	64.8	56.6	64.8	67.9	53.6	69.4 ± 15.2	60.5 ± 3.7
Average (AntMaze)	74.2	69.6	78.3	79.1	73.6	73.8 ± 8.0	66.5 ± 3.8

We observe that GMPG's performance in the AntMaze environment does not surpass that of GMPO, unlike in the locomotion medium and medium-replay tasks. This is particularly evident in the AntMaze medium and large tasks, where the maze size increases and GMPG becomes less effective. This discrepancy may result from the increased complexity and task length of the AntMaze environment, which demands stable and effective policy generation. The goal in this environment is timely navigation through the maze, not rapid completion; faster trajectories do not yield higher rewards. Aggressive strategies can cause ant agents to fall and fail to complete the task, potentially explaining the performance difference between GMPO and GMPG in AntMaze.

D.3 Ablation Experiments

Temperature Coefficient β The temperature coefficient β is a common hyperparameter in both GMPO and GMPG. Larger β values indicate stronger exploration. As shown in Table 12, a moderate β value is beneficial for performance.

Table 12: Performance comparison of temperature coefficient β for GMPO and GMPG.

Algo. / Model type / Function Type	**GMPO / GVP /** $v(x_t, t)$			**GMPG / VPSDE /** $v(x_t, t)$		
Pretrain scheme / Fintune scheme	- / Eq. 40			Eq. 3 / Eq. 8		
β	1	4	8	1	4	8
halfcheetah-medium-v2	43.2 ± 1.2	48.9 ± 1.9	49.9 ± 2.7	57.0 ± 3.1	56.1 ± 2.7	55.5 ± 2.6
halfcheetah-medium-replay-v2	40.6 ± 2.9	42.3 ± 3.6	42.2 ± 3.1	47.1 ± 2.5	50.5 ± 2.7	50.0 ± 3.0

Solver Schemes for Sampling. Table 13 shows the performance comparison of different solver schemes for GMPO and GMPG. We find GMPO and GMPG to be robust to the choice of solver schemes, with performance remaining consistent across different schemes.

Table 13: Performance comparison using different solver schemes for GMPO/GMPG. RK4 stands for the Fourth-order Runge-Kutta with $3/8$ rule. DPM-Solver of order 2 is used for 17 steps sampling. Other solver schemes are used for 32 steps sampling. The average performance is very close across different solver schemes.

Pretrain scheme / Finetune scheme	**GMPO / VPSDE /** $v(x_t, t)$ - / Eq. 40			
Solver schemes	Euler-Maruyama	Midpoint	RK4	DPM-Solver
hopper-medium-v2	78.5 ± 20.2	76.9 ± 20.4	75.0 ± 22.1	76.7 ± 19.2
halfcheetah-medium-expert-v2	89.6 ± 4.3	83.5 ± 8.9	83.6 ± 4.7	90.9 ± 3.6
Pretrain scheme / Finetune scheme	**GMPG / VPSDE /** $v(x_t, t)$ Eq. 3 / Eq. 8			
Solver schemes	Euler-Maruyama	Midpoint	RK4	DPM-Solver
hopper-medium-v2	101.1 ± 2.6	98.3 ± 9.6	98.9 ± 2.1	100.5 ± 2.2
halfcheetah-medium-expert-v2	89.0 ± 6.4	88.2 ± 5.4	88.2 ± 4.3	89.7 ± 4.0

E FRAMEWORK

GenerativeRL is implemented using native *PyTorch 2.0* and utilizes numerical solvers like *torchdiffeq* (Chen et al., 2018) and *Torchdyn* (Poli et al., 2021) for ordinary differential equations. Unlike frameworks such as Hugging Face Diffusers (von Platen et al., 2022) that generate final outputs, in reinforcement learning (RL), generative models act as policies, world models, or other components. This requires a differentiable sampling process with computable and differentiable likelihoods. *GenerativeRL* addresses this by supporting sampling $x \sim p(\cdot|c)$ and computing $\log p(x|c)$ with or without automatic differentiation, uniformly across all continuous-time generative models.

E.1 USAGE EXAMPLE

Figure 4 illustrates a usage example of *GenerativeRL*. The framework is user-friendly and designed for ease of use by reinforcement learning researchers. All models, training, and sampling processes are defined in a single script, simplifying understanding and modifications. Experiment configurations are recorded automatically, facilitating result reproduction.

Modular settings allow users to switch between different generative models, neural network components, and special configurations easily. Once the model is defined, training and sampling require only a few lines of code. Users can switch between training objectives and inference strategies seamlessly. Most functions for generative models support batch processing and automatic differentiation, ensuring smooth integration into reinforcement learning algorithms.

E.2 FRAMEWORK STRUCTURE

The framework structure is illustrated in Figure 5. It consists of three main components: reinforcement learning algorithms, generative models, and neural network components. The reinforcement learning algorithms include those based on generative models, such as QGPO and SRPO. The generative models, including diffusion, flow, and bridge models, are used to model data distributions and serve as key components in RL algorithms. The neural network components comprise commonly used layers like DiT and U-Net, which are essential for building generative models. Users can customize the neural network components and generative models to fit their specific needs. The framework is designed to be compatible with future RL algorithms and can be easily extended for different RL tasks.

The currently supported generative models are listed in Table 14.

Table 14: Models functionality in *GenerativeRL*

Name	Score Matching	Flow Matching	$x \sim p(\cdot)$	$x \sim p(\cdot\|c)$
Diffusion models				
VPSDE	✓	✓	✓	✓
GVP	✓	✓	✓	✓
Linear (Karras et al., 2022)	✓	✓	✓	✓
Flow models				
I-CFM	✗	✓	✓	✓
OT-CFM (Tong et al., 2024)	✗	✓	✓	✗
Bridge models				
SF2M (Tong et al., 2023)	✗	✗	✓	✗

✓ Supported. ✗ Not supported.

F Limitations and Future Work

Our work has several limitations:

- We focused on policy extraction using an optimal Q-value function trained with IQL, without considering suboptimal Q-value functions or improving Q-value estimation using generative models. This remains an open question for actor-critic methods utilizing generative models as policies.
- Generative models excel in high-dimensional data generation but may perform similarly to discriminative models in low-dimensional contexts. Since most RL environments are low-dimensional, future work should explore environments like Evogym (Bhatia et al., 2021), where generative policies can leverage larger action spaces.
- We did not address scenarios where generative policies are deployed online with real-time data generation. Future studies should assess the stability of policy optimization in dynamic data contexts, evaluate performance, and consider the additional costs of using generative policies.

G Societal Impacts

This work uses generative models as policy models in reinforcement learning, applicable in real-world applications such as robots and autonomous vehicles. Given uncertainties in Q-value function training and reward labeling, potential negative societal impacts exist, including the risk of aligning generative models with harmful Q-value functions. Therefore, caution is essential throughout the training and deployment process, from data collection and reward labeling to Q-value function training and the application of generative policies. Additionally, we must prevent the abuse of this technology, such as using it for illegal activities or unethical purposes.

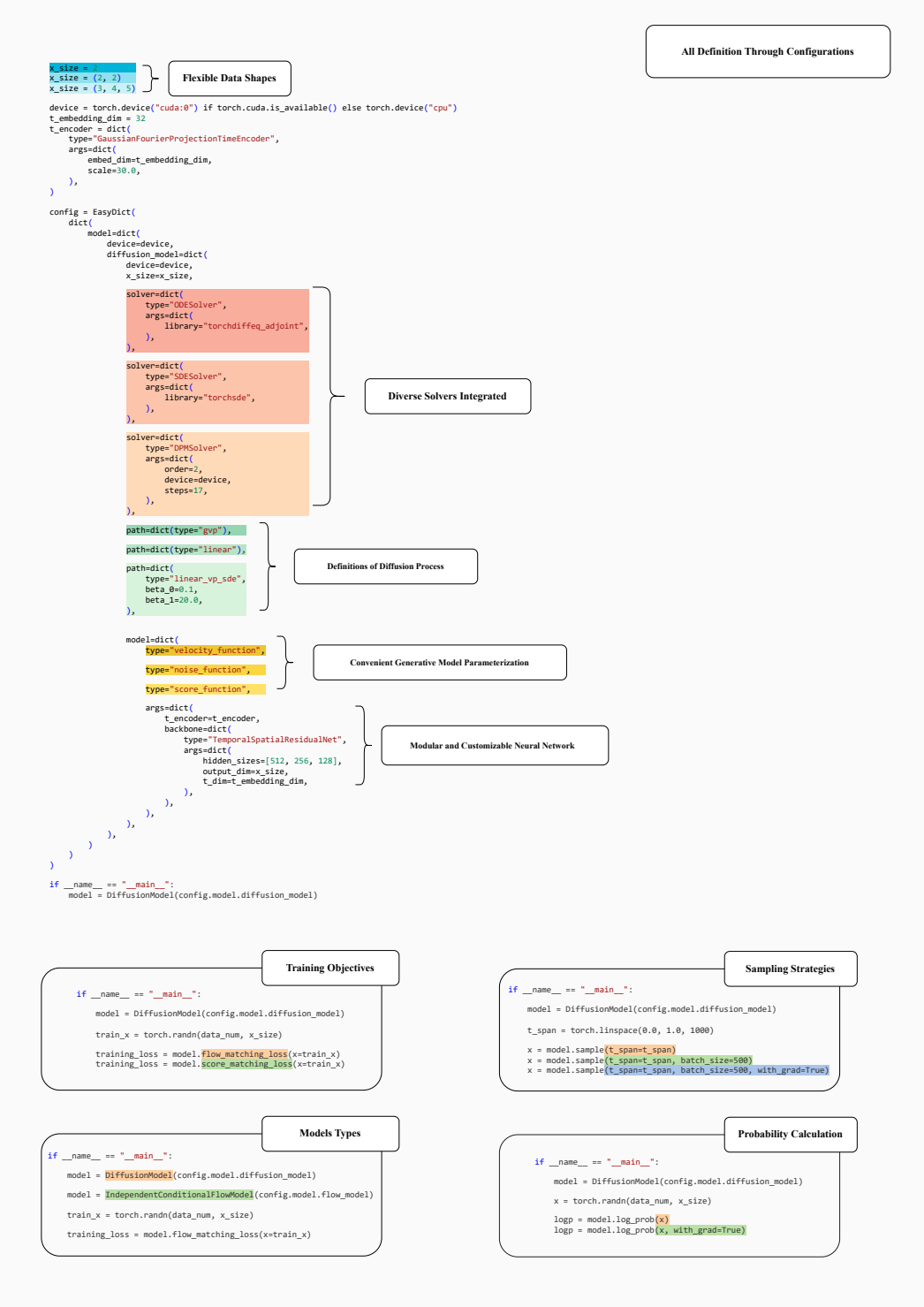

Figure 4: An example of using *GenerativeRL* for defining models, training, and sampling. All experiment configurations are orgnized in a nested dictionary and can be recorded for reproductions. Configuration of every component is modular and can be easily switched. Diverse generative models and neural network components are supported. User can switch between training objectives and inference strategies easily. Most functions support batch processing and automatic differentiation with only a few lines of code. This configuration is flexible and can be easily extended for different RL tasks.

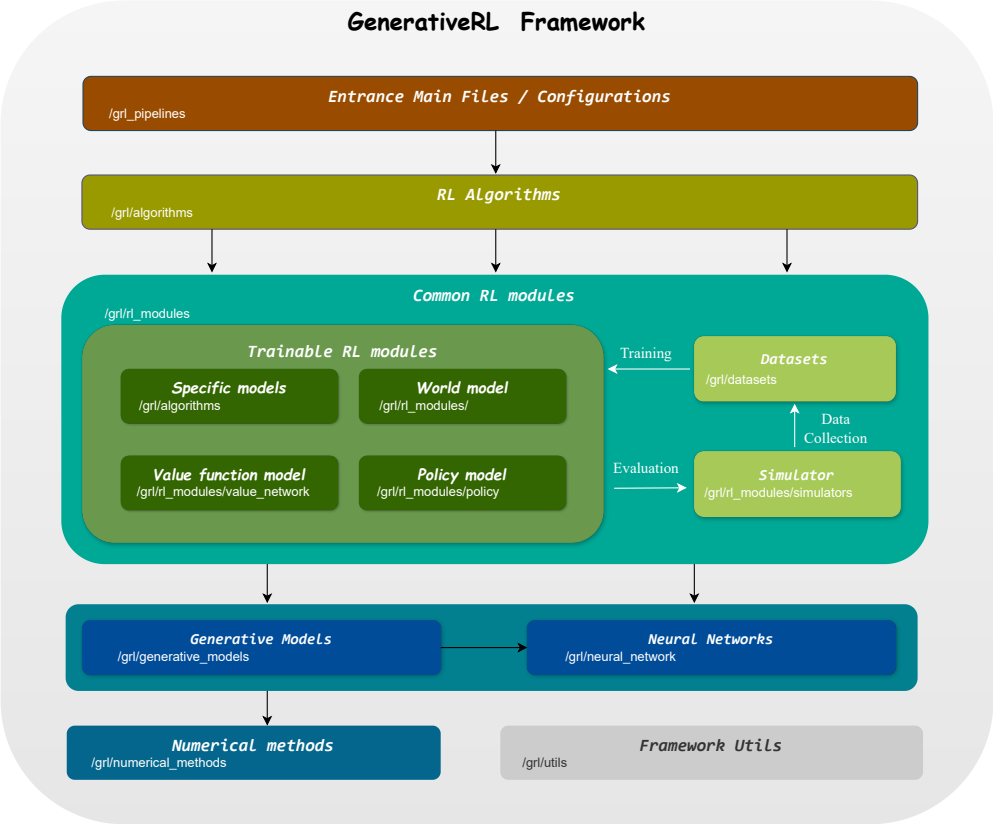

Figure 5: Framework structure of *GenerativeRL*.